

# Genesis of flood basalts and Basin and Range volcanic rocks from Steens Mountain to the Malheur River Gorge, Oregon

Victor E. Camp<sup>†</sup>

*Department of Geological Sciences, San Diego State University, San Diego, California 92181, USA*

Martin E. Ross

*Department of Geology, Northeastern University, Boston, Massachusetts 02115, USA*

William E. Hanson

*Department of Geological Sciences, San Diego State University, San Diego, California 92181, USA*

## ABSTRACT

The middle and south forks of the Malheur River provide a unique mapping corridor connecting two flood-basalt successions—Steens basalt to the south and the basalt of Malheur Gorge to the north. Each contains chemically defined subtypes, which merge stratigraphically across the north-south length of the map area. The lowermost flows of Steens basalt are stratigraphically equivalent to the lowermost flows of the basalt of Malheur Gorge. The uppermost flows of Steens basalt pinch out in the map area, but are partly interbedded with the middle and uppermost flows of the basalt of Malheur Gorge, which continue to thicken northward. The upper part of the tholeiitic succession is interbedded with a group of previously unrecognized lavas—the Venator Ranch basalt flows. Tholeiitic volcanism ceased at ca. 15.3 Ma; the last tholeiitic unit that erupted is the Hunter Creek basalt, which also thickens northward.

Subsequent (younger than 15.3 Ma), more localized eruptions were dominated by calc-alkaline to mildly alkaline lavas associated with Basin and Range extension. Local uplift generated deep canyons, which were filled by andesitic lavas of the Keeney sequence (ca. 13–10 Ma). The final eruptive products include the Devine Canyon tuff (ca. 9.7 Ma), the Drinkwater basalt (ca. 6.9 Ma), and the Voltage flow (older than 32,000 yr B.P.).

Major and trace element analyses demonstrate that (1) crystal fractionation was a

universal process in the derivation of the tholeiitic lavas, (2) the diverse Steens basalt and basalt of Malheur Gorge chemical subtypes were further modified by variations in the degree of partial melting, mantle-source composition, crustal contamination, and/or magma mixing, (3) the Keeney sequence lavas show little evidence of crystal fractionation, but instead were derived from the mixing of basaltic melts with high-silica, low-Fe, granitic sources, and (4) the felsic rock types were derived from the anatexis of heterogeneous crustal sources.

Stratigraphic correlations demonstrate that the main phase of middle Miocene flood-basalt volcanism generated ~220,500 km<sup>3</sup> of basalt over an interval of ~1.3 m.y., which equates to a magma supply rate of 0.17 km<sup>3</sup>/yr. The rapid accumulation of lava appears to have been contemporaneous with a markedly consistent, northward propagation of regional uplift, basalt regression, and vent migration across the breadth of eastern Oregon and into southeastern Washington. The northward advancement of volcanism and uplift may represent the surface expression of a spreading mantle plume head, deflected against the thick cratonic margin of North America and channelized beneath a thin oceanic lithosphere of accreted terranes.

**Keywords:** Basin and Range province, flood basalt, Oregon, mantle plume, Steens basalt, Columbia River basalt.

## INTRODUCTION

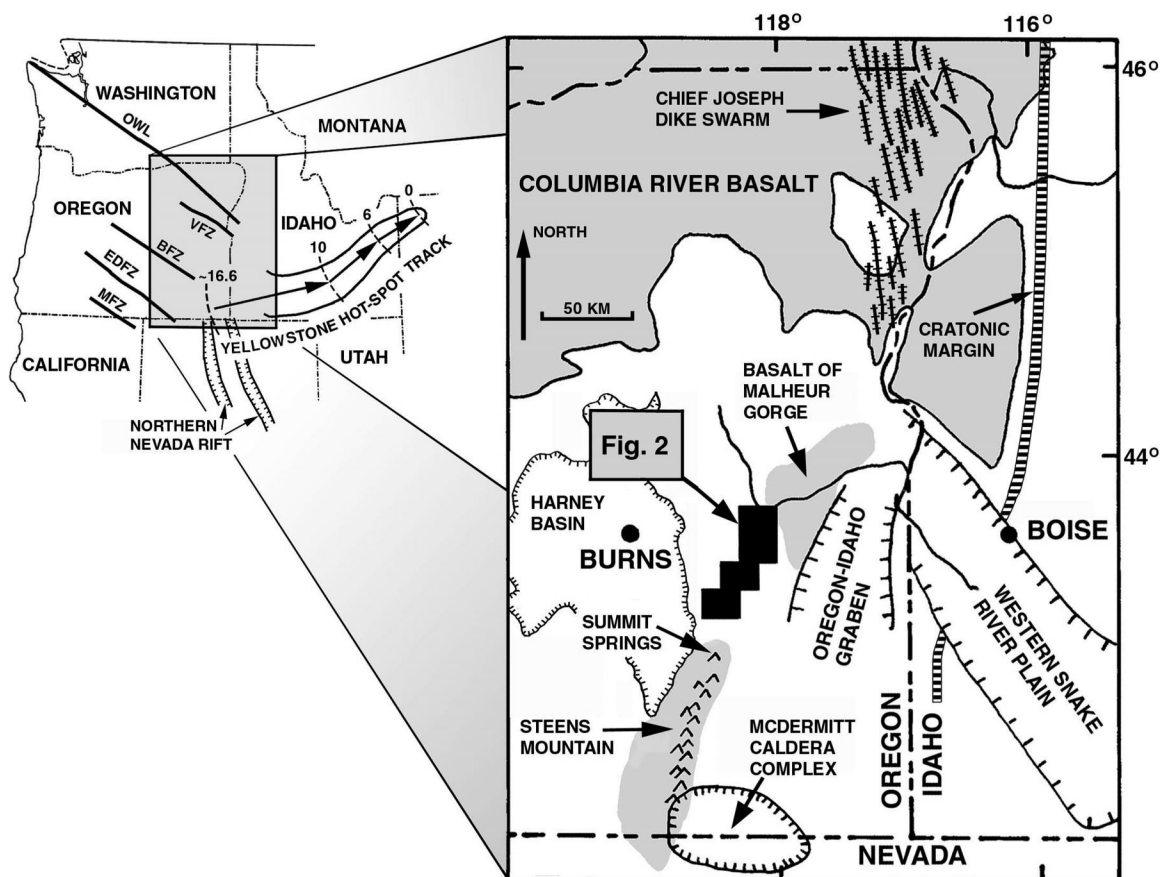
The Cenozoic volcanic stratigraphy of eastern Oregon is constructed on a pre-Tertiary

basement of accreted oceanic terranes that are juxtaposed against the North American Precambrian craton to the east (Vallier, 1995). The basement rocks become more transitional in character, and isotopically more evolved, toward the cratonic boundary (Armstrong et al., 1977; Kistler and Peterman, 1978; Leeman et al., 1992). This relatively thin transitional to oceanic lithosphere was subjected to at least three phases of Tertiary extension and magmatism, reflected in a regionally extensive tripartite stratigraphy lying above the pre-Tertiary basement. From oldest to youngest, the stratigraphic divisions are as follows: (1) a widespread, but poorly exposed, assemblage of calc-alkaline lavas and pyroclastic rocks that are mainly Oligocene to early Miocene in age (Walker, 1977; Robinson et al., 1990), (2) a voluminous succession of middle Miocene tholeiitic flood-basalt lavas of the Steens basalt and Columbia River Basalt Group, and (3) a widespread but disseminated suite of calc-alkaline to mildly alkaline lavas, pyroclastic rocks, and felsic intrusions related to the middle Miocene to Holocene development of the northern Basin and Range province. The Basin and Range stratigraphy is also associated with high-alumina olivine tholeiites (HAOT), which began to erupt on the Oregon Plateau at ca. 10.5 Ma (Hart et al., 1984).

There has been much debate on the genesis and possible interrelationships of these stratigraphic assemblages. Eaton (1984), Carlson and Hart (1987), and Hart and Carlson (1987), for example, have suggested that backarc extension has been the dominant mechanism for mafic to bimodal volcanism on the Oregon Plateau over the past 17 m.y. Several other workers have suggested instead that emplacement of the Yellowstone mantle plume near

<sup>†</sup>E-mail: vcamp@geology.sdsu.edu.

Figure 1. The map area lies in eastern Oregon, midway between the Harney Basin to the west and the Oregon-Idaho graben to the east. It separates the tholeiitic basalt exposures of Steens Mountain to the south from the canyon-land exposures of the basalt of Malheur Gorge to the north. The Precambrian cratonic margin of North America, defined by the Mesozoic  $^{87}\text{Sr}/^{86}\text{Sr} = 0.706$  line of Leeman et al. (1992), separates the older, thicker craton to the east from a Mesozoic basement of accreted oceanic terranes to the west. The pre-Tertiary oceanic basement is transected by Columbia River basalt feeder dikes



of the Chief Joseph dike swarm in the north and is overlain, in part, by Steens basalt and the basalt of Malheur Gorge in the south. Northwest-trending fault zones: OWL—Olympic-Wallowa Lineament; VFZ—Vale fault zone; BFZ—Brothers fault zone; EDFZ—Eugene-Denio fault zone; MFZ—McLaughlin fault zone. Migration of the Yellowstone mantle plume through time is denoted by the progressive age designations (in Ma) along the Yellowstone hotspot track.

the Oregon-Nevada border resulted in the onset of flood-basalt volcanism at ca. 17 Ma (Brandon and Goles, 1988; Hooper and Hawkesworth, 1993; Dodson et al., 1997; Takahashi et al., 1998). Going still further, Draper (1991), Pierce and Morgan (1992), and Murphy et al. (1998) have suggested that plume emplacement might have been the root cause for both flood-basalt volcanism and subsequent extension associated with the northern Basin and Range province. In contrast, Hooper et al. (2002a) have suggested that plume-generated flood-basalt volcanism was superimposed upon a separate and long-lived period of Basin and Range extension, thus accounting for the entire tripartite stratigraphy. An alternative view is presented by Dickinson (1997), who has suggested that both the flood-basalt volcanism and Basin and Range extension were related to upper-mantle convection induced by torsional stress of the plate interior when the San Andreas fault was fully integrated as a coherent plate boundary.

Although these competing regional models

have generally been well constrained by the results of field investigations across much of the southeastern Columbia Plateau (e.g., Swanson et al., 1979, 1980, 1981; Camp, 1981; Camp and Hooper, 1981; Hooper and Camp, 1981; Reidel et al., 1989; Tolan et al., 1989; Hooper, 1997), their parameters are less well defined by a general dearth of such investigations across significant parts of the Oregon Plateau, which is geologically more complex. The Vale and Mahogany Mountain 1:100,000-scale map sheets (Ferns et al., 1993a, 1993b) are the only regional compilations of 7.5-minute quadrangle maps currently available for southeastern Oregon. The synthesized field data from these maps has led to the identification of the Oregon-Idaho graben (Fig. 1), an important zone of synvolcanic rifting that formed adjacent to the Precambrian cratonic margin from ca. 15.5 to 10.5 Ma. (Cummings et al., 2000).

The credibility of petrogenetic and tectonic models for the northern Basin and Range province requires a more thorough under-

standing of the map distribution, structure, and stratigraphic relationships of the eastern Oregon volcanic rocks. To help fill this apparent gap, we present here new stratigraphic and petrochemical data derived from geologic mapping across eight 7.5-minute quadrangles along the middle and south forks of the Malheur River Gorge, located midway between the Harney Basin to the west and the Oregon-Idaho graben to the east (Figs. 1 and 2). A critical feature of this well-exposed area is that it provides a unique mapping corridor transecting tholeiitic lavas of Steens basalt in the south and the basalt of Malheur Gorge in the north (Fig. 1). The latter is stratigraphically equivalent to the main phase of the Columbia River Basalt Group. With the intent of providing additional constraints on the tectonomagmatic development of the northern Basin and Range province, we examine here stratigraphic correlations between these tholeiitic successions and present new field and petrochemical data on both the middle Miocene tholeiites

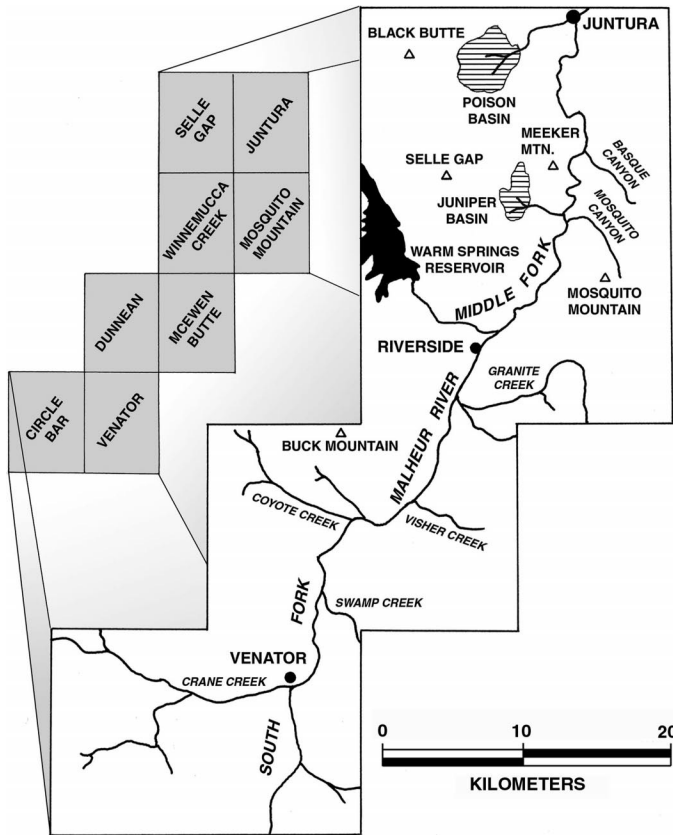


Figure 2. The map area is composed of eight 7.5-minute quadrangles (shaded) lying on opposing sides of the middle and south forks of the Malheur River Gorge. Marked locations and physiographic features are described in the text.

and the overlying late Miocene–Pleistocene volcanic assemblage.

### ASPECTS OF THE GENERAL GEOLOGY

Before describing the Cenozoic volcanic succession, we describe here three important aspects of the general geology (Fig. 3): (1) the overall fault pattern, (2) an undifferentiated group of pyroclastic rocks and pyroclastic sediments, and (3) a variety of shallow, felsic intrusions and rhyolitic eruptive centers.

#### Fault Pattern

The regional geology is transected by a dominant set of northwest-striking faults, a subordinate set of north-striking faults, and sparse east-northeast-striking faults (Fig. 3A). The northwest-trending set lies parallel to a group of major fault zones cutting across southeastern Oregon (Fig. 1) (Lawrence, 1976). Hooper et al. (2002b) suggested that these large fault zones are regions of right-lateral shear and that both of the main fault sets were generated by east-west Basin and Range extension that began after the main period of tholeiitic flood-basalt volcanism. The initial burst of extension appears to be associated with the initial opening of the Oregon-Idaho graben between ca. 15.5 and ca. 13.5 Ma (Cummings et al., 2000).

The two main fault sets are composed of normal faults; the northwest-trending faults generally have greater vertical displacements.

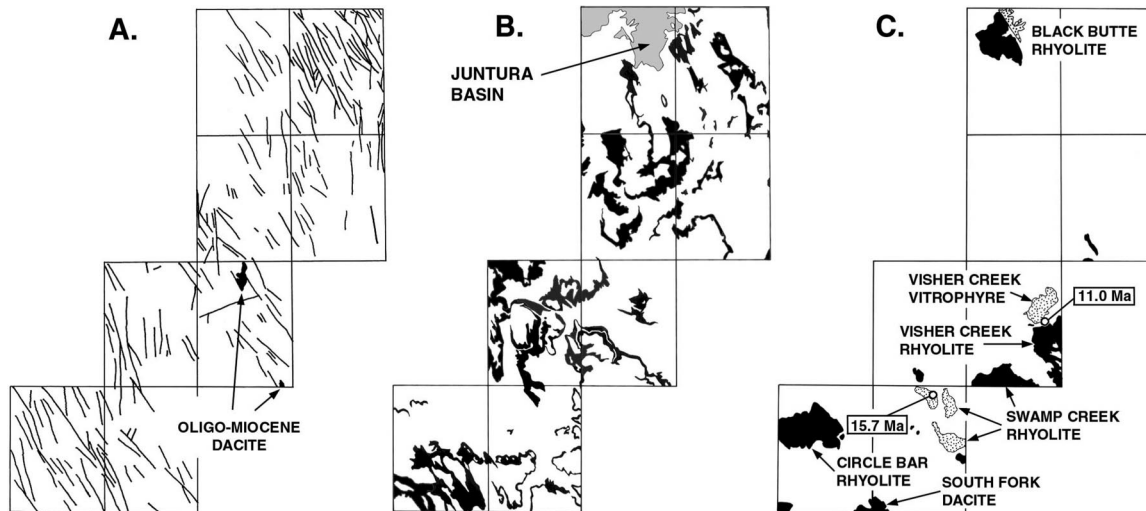


Figure 3. Aspects of the general geology. (A) Overall fault pattern and distribution of the Oligocene–Miocene volcanic rocks. (B) Distribution of the undifferentiated Miocene pyroclastic rocks and pyroclastic sediments, spanning an age range from ca. 15.0 and 7.0 Ma. (C) Distribution of the shallow felsic eruptive centers. Outflow facies of ignimbrite or vitrophyric lava are shown by dotted pattern. Radiometric dates for the Swamp Creek and Visher Creek rhyolites are from Walker (1979).

We found lateral slickensides, however, on a single northwest-trending fault exposed along Shumway grade, 4.5 km east-southeast of Juntura (Fig. 2). Whether the displacement along this fault is right-lateral or left-lateral remains unclear. Faults from the two main trends offset one another, suggesting that they are at least partly contemporaneous. Although both fault sets cut across all Miocene rocks, they are much less common in the late Miocene olivine basalt remnants (ca. 7.0 Ma) that cap the more highly deformed middle Miocene stratigraphy. The field data suggest that both sets of faults may have been reactivated several times throughout the middle to late Miocene.

### Undifferentiated Miocene Pyroclastic Rocks and Pyroclastic Sediments

The Miocene volcanic stratigraphy contains numerous semiconsolidated deposits of felsic ash, air-fall pumice deposits, and tuffaceous sediment. On a local scale, the relative ages of these deposits are well defined by stratigraphic marker beds. On a more regional scale, however, this stratigraphic control becomes more elusive owing to lateral facies changes within the volcanoclastic stratigraphy combined with the pinching out of most marker beds across the map area. Therefore, we have combined most of these units into a single, undifferentiated unit of Miocene pyroclastic rocks and pyroclastic sediments (Fig. 3B), which spans an age range between ca. 15.5 Ma (where they lie above tholeiitic flood basalts) and ca. 7.0 Ma (where they lie beneath late Miocene diktytaxitic olivine basalts). The thickest accumulation of these semiconsolidated tuffaceous rocks lies above the basalt of Malheur Gorge in the Juntura Basin, in the northwestern part of the map area (Fig. 3B). Farther to the northwest, the upper part of this volcanoclastic succession contains abundant white diatomite and lacustrine sediments with plant and vertebrate fossils of late Miocene to early Pliocene age (Greene et al., 1972; Johnson et al., 1998b). Although most of the pyroclastic air-fall deposits are likely to have had local sources, it is not inconceivable that some of the finer ash-fall deposits were derived from explosive, Plinian-type eruptions associated with the Cascade volcanic arc.

### Shallow Felsic Eruptive Centers

The Miocene volcanic stratigraphy is intruded by a number of dacitic to rhyolitic volcanic centers (Fig. 3C), some of which contain ring dikes and outflow facies of ignimbrite, rheomorphic ignimbrite, or vitrophyric lava

(Fig. 3C). Field data, together with two K-Ar dates, partly define the relative ages of the eruptive centers. For example, outflow facies of the Swamp Creek and Visher Creek rhyolites (Fig. 3C) unconformably overlie tholeiitic lavas of Steens basalt (ca. 16.6–15.3 Ma). The Visher Creek rhyolite appears to be the younger of the two, with a reported K-Ar age of 11.0 Ma (Walker, 1979). A significantly older age for the Swamp Creek rhyolite is indicated by an obsidian clast of Swamp Creek chemistry that was sampled from a reworked volcanoclastic unit lying beneath the ca. 15.3 Ma Dinner Creek tuff (Fig. 4). This field evidence indicates that the Swamp Creek eruptive center was active during the later stages of flood-basalt volcanism, a relationship consistent with a reported K-Ar age of 15.7 Ma for a small vitrophyric outlier of the Swamp Creek rhyolite in the northern part of the McEwen Butte Quadrangle (Walker, 1979).

The relative age of the Black Butte eruptive center, in the northern part of the map area (Fig. 3C), is based on the deposition of an ignimbritic outflow facies above the upper part of the Juntura Basin stratigraphy. This relationship indicates that Black Butte was active in the late Miocene (after 13.0 Ma), contemporaneous with eruption of intermediate to felsic, calc-alkaline volcanic rocks found throughout the map area.

It seems reasonable to conclude that the rhyolitic centers identified in Figure 3C may have been active at various times from ca. 15.7 Ma to ca. 7.0 Ma, potentially providing a significant source for the felsic ash and pumiceous air-fall deposits found in both the Miocene undifferentiated unit described in the previous section, and the Kool Spring formation described in the following section.

## VOLCANIC STRATIGRAPHY

The Cenozoic stratigraphy exposed along the middle and south forks of the Malheur River Gorge is subdivided here into five, petrochemically distinct volcanic successions, separated from one another by well-developed unconformities (Fig. 4): (1) Oligocene–Miocene calc-alkaline dacite, (2) mafic to bimodal rocks associated with the middle Miocene period of tholeiitic flood-basalt volcanism (ca. 16.6–15.3 Ma), (3) early diktytaxitic olivine basalts (ca. 13.5 Ma), (4) calc-alkaline, intermediate to felsic rocks associated with Basin and Range extension (ca. 13.0–9.7 Ma), and (5) late diktytaxitic olivine basalts (ca. 7 Ma to ca. 32,000 yr B.P.).

### Oligocene–Miocene Calc-Alkaline Dacite

We have identified two small exposures of high-silica dacite in the McEwen Butte Quadrangle that predate rocks of the tholeiitic assemblage (Figs. 2 and 3A). The largest exposure is intruded by dikes (Fig. 5) of tholeiitic basalt (Venator Ranch chemical type; see next section) and unconformably overlain by the tholeiitic basalt-bearing Kool Spring formation (see next section). Similar outcrops of late Oligocene–early Miocene calc-alkaline volcanic rocks are found beneath the flood-basalt succession at small, scattered locations throughout southeastern Oregon and adjacent Idaho (Ekren et al., 1981; Walker and MacLeod, 1991). These include lava and pyroclastic sequences at the base of Steens Mountain, ~50 km south of the map area (Langer, 1991), at Beulah Reservoir, ~25 km north of the map area (M.L. Cummings, 2000, personal commun.), and at Unity Reservoir, ~100 km north of the map area (Brooks et al., 1979). Radiometric dates from the calc-alkaline sequence beneath the tholeiitic basalts at Steens Mountain vary from 23.7 Ma to 17.8 Ma (Laursen and Hammond, 1974; Hart and Carlson, 1985; Langer, 1991; A. Grunder, 2001, personal commun.).

### Mafic to Bimodal Volcanic Rocks Associated with Tholeiitic Flood-Basalt Volcanism

The age range of tholeiitic flood-basalt volcanism in the map area appears to be fairly well established by  $^{40}\text{Ar}/^{39}\text{Ar}$  radiometric dates from both Steens basalt to the south and the basalt of Malheur Gorge to the north and northeast. To the south, Swisher et al. (1990) reported  $^{40}\text{Ar}/^{39}\text{Ar}$  ages of  $16.58 \pm 0.005$  Ma for the uppermost flow at Steens Mountain and  $16.59 \pm 0.02$  Ma for the thirty-first flow from the top. Less precise data on lower flows indicated similar ages (Baksi et al., 1991). Brueseke and Hart (2000) presented twelve  $^{40}\text{Ar}/^{39}\text{Ar}$  dates for Steens-type basalt flows from near Steens Mountain that yielded a range of ages from  $16.46 \pm 0.14$  to  $15.06 \pm 0.26$  Ma.

To the north, Hooper et al. (2002a) subdivided the basalt of Malheur Gorge into three stratigraphic and compositional units, with the following weighted mean  $^{40}\text{Ar}/^{39}\text{Ar}$  ages: lower Pole Creek basalt ( $16.9 \pm 0.8$  Ma), upper Pole Creek basalt ( $16.5 \pm 0.3$  Ma), and Birch Creek basalt ( $15.7 \pm 0.01$  Ma). Tholeiitic volcanism continued, however, with eruption of the Hunter Creek basalt, which is interbedded in a sequence of essentially contemporaneous

VOLCANIC SUCCESSION		VOLCANIC UNIT	AGE	COMMENT
Late Diktytaxitic Olivine Basalts		Voltage flow	32 ka	A
		Drinkwater basalt	ca. 7.0 Ma	B
<i>Regional Unconformity</i>				
Intermediate to Felsic Calc-alkaline Rocks	KEENEY SEQUENCE	Devine Canyon tuff	ca. 9.7 Ma	C
		Cobb Creek lavas	—	—
		Riverside lavas	10.14 ± 0.23 Ma	D
		Buck Mtn. lavas	12.5 ± 0.5 Ma	E
<i>Regional Unconformity</i>				
Early Diktytaxitic Olivine Basalts		Tims Peak basalt	13.5 ± 0.1 Ma	F
<i>Regional Unconformity</i>				
Tholeiitic Mafic to Bimodal Rocks		Hunter Creek basalt	15.3 ± 0.1 Ma	F,G
		Dinner Creek tuff		
		Kool Spring fm.	—	—
		Steens basalt, Venator Ranch basalt, and basalt of Malheur Gorge	15.7 ± 0.1 Ma	F,G
<i>Regional Unconformity</i>				
			16.6 ± 0.02 Ma	H
Oligo-Miocene dacite			ca. 23.7-17.8 Ma	I

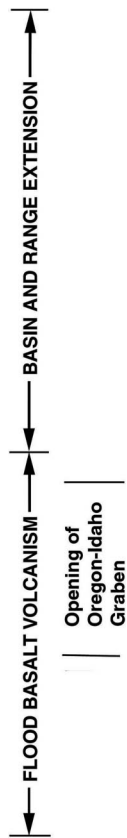


Figure 4. The Cenozoic stratigraphy along the middle and south forks of the Malheur River, Oregon, is subdivided here into five volcanic successions separated by well-developed unconformities. Comments on age designations: (A) Gehr and Newman (1978). (B) Greene et al. (1972). (C) <sup>40</sup>Ar/<sup>39</sup>Ar age of Streck et al. (1999). (D) This study. (E) This tentative age estimate of the Buck Mountain lavas is based on their chemical similarity to a group of lavas mapped as Shumway basalt, dated by Fiebelkorn et al. (1983). (F) Weighted mean of <sup>40</sup>Ar/<sup>39</sup>Ar ages from Hooper et al. (2002a). The 13.4 Ma age for Tims Peak basalt is the weighted mean of four <sup>40</sup>Ar/<sup>39</sup>Ar ages ranging from 13.9 to 13.1 Ma for the Hat Top and Prava Peak chemical types. These types are not present in the map area. We infer that it is likely that the age range for these various eruptions is larger than this single date indicates, falling somewhere between the weighted mean ages of Hunter Creek basalt at 15.3 Ma and the early Keeney sequence flows at ca. 13 Ma. The 15.7 Ma age for the upper part of the tholeiitic succession is the weighted mean of three Birch Creek lavas from Hooper et al. (2002a). (G) The <sup>40</sup>Ar/<sup>39</sup>Ar ages of Brueseke and Hart (2000) are similar to those of Swisher et al. (1990) and Hooper et al. (2002a); however, their youngest age suggests that tholeiitic volcanism south of the map area may be as young as 15.06 ± 0.26 Ma. (H) <sup>40</sup>Ar/<sup>39</sup>Ar ages of Swisher et al. (1990). These are similar to the weighted mean averages of Hooper et al. (2002a) for the lower and upper Pole Creek basalts. (I) Range of dates from volcanic rocks that predate the Steens basalt and occur at the base of Steens Mountain (Laurson and Hammond, 1974; Hart and Carlson, 1985; Langer, 1991; A. Grunder, 2001, personal commun.).

felsic tuffs, ignimbrites, and rhyolitic lavas referred to by Lees (1994) and Hooper et al. (2002a) as the Hog Creek sequence. They presented ten <sup>40</sup>Ar/<sup>39</sup>Ar ages for the Hog Creek sequence, with a weighted mean of 15.3 Ma ± 0.1 Ma. The Hunter Creek basalt lies directly above the Dinner Creek tuff, a rhyolitic ignimbrite at the base of the Hog Creek sequence, which has also been dated at 15.3 Ma (Laurson and Hammond, 1974; Hooper et al.,

2002a). We are in general agreement with Hooper et al. (2002a) that tholeiitic volcanism began at ca. 16.6 Ma and continued until ca. 15.3 Ma (Fig. 4), with the possible exception of an unknown volume of slightly younger Steens-type eruptions from near the vicinity of Steens Mountain (Brueseke and Hart, 2000).

The middle Miocene interval of flood-basalt volcanism is characterized by stratigraphic variations across the north-south length of the

map area. Figure 6 is a schematic depiction of these lateral facies changes, from the Summit Springs stratigraphic section ~13 km south of the map area (Fig. 1), through the Venator to Riverside region in the south and central part of the map area (Fig. 2), to the Juntura region in the north. Throughout most of this region, the upper part of the Steens sequence is interbedded with a group of previously unrecognized tholeiitic lavas, herein referred to as the

Figure 5. Dike of Venator Ranch basalt cutting across Oligocene–Miocene volcanic rocks in the McEwen Butte Quadrangle, 7 km south of Riverside, Oregon.

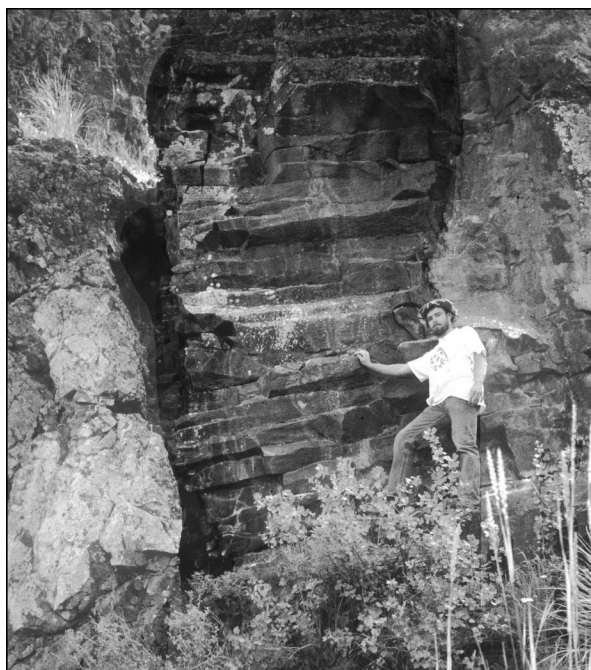
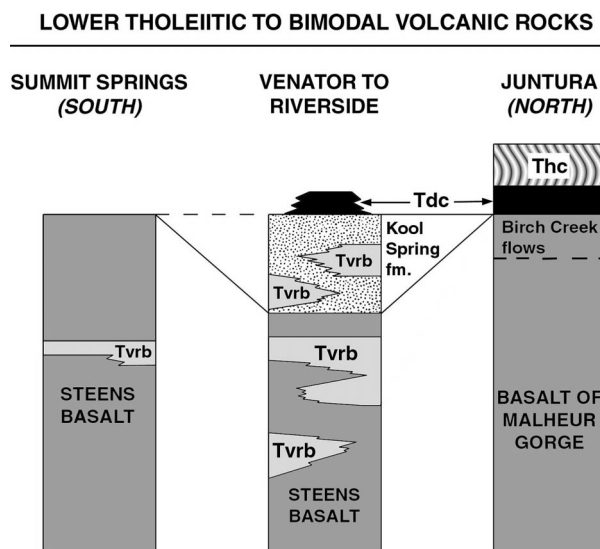


Figure 6. Schematic stratigraphic columns showing the relationship of the Venator Ranch lavas and the Kool Spring formation to the Steens basalt stratigraphy, exposed in the Summit Springs section to the south, and the basalt of Malheur Gorge stratigraphy, exposed in the Juntura Quadrangle to the north. Tvr<sub>b</sub>—Venator Ranch basalt, Tdc—Dinner Creek tuff, and Thc—Hunter Creek basalt.



Venator Ranch basalt. The interbedded succession of Steens and Venator Ranch basalts is in turn overlain by an interbedded bimodal succession of air-fall pyroclastic deposits and Venator Ranch basalt flows, herein called the Kool Spring formation (Figs. 4). Two small outcrops of the Dinner Creek tuff overlie the Kool Spring formation in the northeast corner of the Circle Bar Quadrangle, ~3 km west-northwest of Venator (Fig. 2). This stratigraphic relationship demonstrates that at least part of the Kool Spring formation was deposited before ca. 15.3 Ma. The final eruptive product of tholeiite volcanism is the Hunter Creek basalt, which overlies the Dinner Creek

tuff in the northeastern part of the map area. The map distribution of the entire mafic to bimodal succession is shown in Figure 7, and a more thorough description of each unit is presented in the next section.

#### *Correlation of Steens Basalt and the Basalt of Malheur Gorge*

A comparison of ~700 major and trace element analyses from Steens basalt, the basalt of Malheur Gorge, and Columbia River Basalt Group, led Binger (1997) to conclude that (1) lower Pole Creek lavas (basalt of Malheur Gorge) are chemically indistinguishable from Steens basalt exposed in the lower part of the

Steens Mountain section (Johnson et al., 1998a), (2) upper Pole Creek lavas (basalt of Malheur Gorge) are indistinguishable from Imnaha Basalt (Columbia River Basalt Group), and (3) Birch Creek and Hunter Creek lavas (basalt of Malheur Gorge) are indistinguishable from Grande Ronde Basalt (Columbia River Basalt Group). The upper flows in the Steens Mountain section have some similarities to the Birch Creek and Grande Ronde lavas, but are chemically distinct (Johnson et al., 1998a).

The lower part of the tholeiitic succession exposed both at Steens Mountain and in the Malheur River Gorge is more primitive than the upper part (Lees, 1994; Johnson et al., 1998a; Binger, 1997). In the map area between these two regions, we have analyzed 60 samples that fall along the Steens basalt–basalt of Malheur Gorge trend lines. Some are chemically equivalent to primitive lavas of lower Steens basalt, and a few others are chemically equivalent to more evolved lavas of Birch Creek basalt. Most of the analyses, however, fall along trends that are transitional between upper Steens basalt and upper Pole Creek basalt, without any clear distinction between the two. These transitional lavas provide a chemical link consistent with a progressive geographic change in chemical composition during contemporaneous or overlapping eruption of upper Steens basalt to the south and upper Pole Creek basalt to the north.

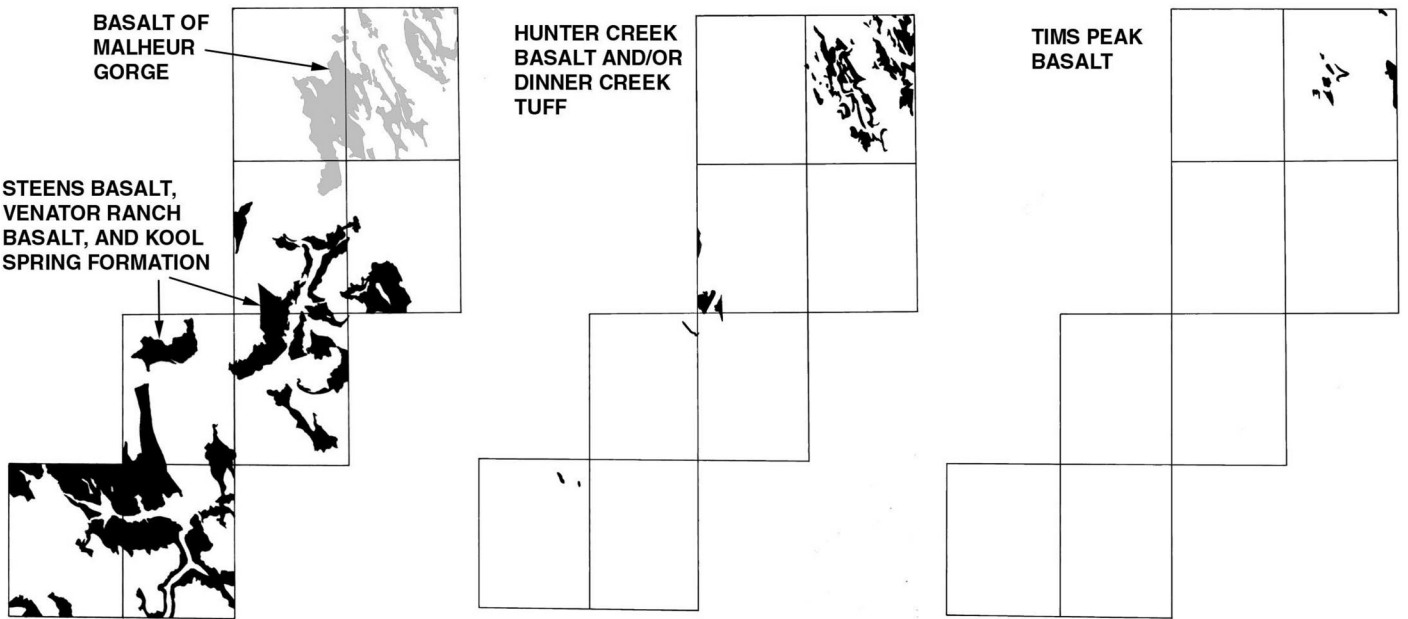
This chemical link is verified by map correlations showing a physical link between Steens basalt and the basalt of Malheur Gorge (Camp and Ross, 2000). We have now identified and mapped Steens basalt flows extending from the northernmost outlier of Steens Mountain (the Summit Springs section, Fig. 1), northward through the map area, to within 5 km of the southernmost outcrops of the basalt of Malheur Gorge exposed in the Juntura and Winnemucca Creek Quadrangles (Figs. 2 and 7). Here, an overlying assemblage of canyon-filling lavas (the Keeney sequence, Fig. 4) prevents a direct physical connection of these tholeiitic outcrops. Their stratigraphic position and their overall chemical similarity, however, provide clear evidence that Steens basalt and the basalt of Malheur Gorge are correlative units (Camp and Ross, 2000).

#### *Venator Ranch Basalt and the Kool Spring Formation*

Although the Venator Ranch basalt flows are chemically similar to the Steens basalt–basalt of Malheur Gorge lavas, they can be readily distinguished by their trace element compositions, and most notably by their lower

**MAFIC TO BIMODAL ROCKS ASSOCIATED WITH FLOOD-BASALT VOLCANISM (16.6 to 15.3 Ma)**

**EARLY DIKTYTAXITIC OLIVINE BASALTS (ca. 13.5 Ma)**



**INTERMEDIATE TO FELSIC ROCKS ASSOCIATED WITH BASIN AND RANGE EXTENSION (ca. 13.0 - 9.7 Ma)**

**LATE DIKTYTAXITIC OLIVINE BASALTS (ca. 7 Ma to ca. 32,000 B.P)**

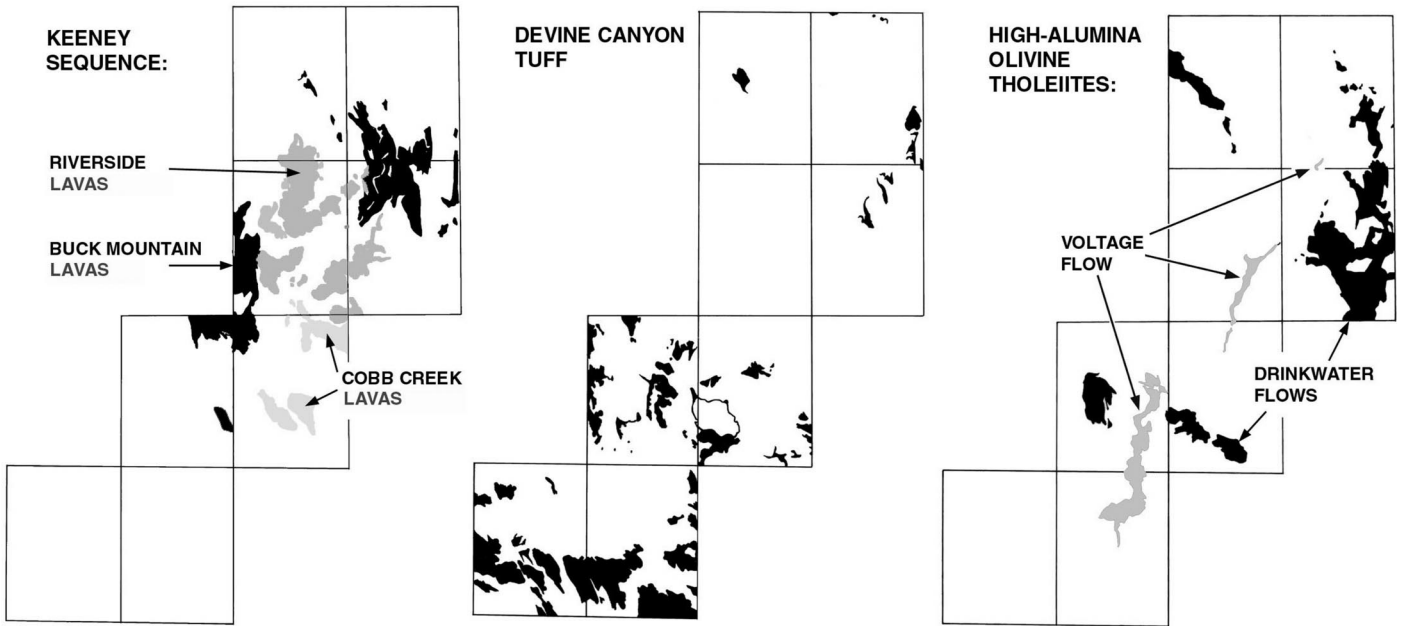


Figure 7. Map distribution of Miocene–Holocene lava flows, flow sequences, and ignimbrites.

TiO<sub>2</sub>/P<sub>2</sub>O<sub>5</sub> ratios (see Chemical Correlations section). By using these criteria, we have identified at least one Venator Ranch basalt flow (JS-32) in the ~900-m-thick Steens Mountain section (Johnson et al., 1998a). The four uppermost flows at Steens Mountain also have TiO<sub>2</sub>/P<sub>2</sub>O<sub>5</sub> ratios similar to those of the Venator Ranch basalt, but they are more evolved and display dissimilar incompatible element ratios. About 50 km farther north, we have identified four Venator Ranch basalt flows (CR109, CR111–CR113; GSA Data Repository<sup>1</sup>) in the upper half of the 300-m-thick Summit Springs section (Fig. 1). Still farther north, into the southern and central parts of the map area, Venator Ranch lavas become abundant. Here, they are interbedded with Steens basalt, becoming more prevalent in the upper part of collected sections.

Both Steens and Venator Ranch lavas are overlain by the Kool Spring formation. This bimodal succession is composed of felsic air-fall pyroclastic rocks and pyroclastic sediments, interbedded Venator Ranch basalt flows, and locally interbedded basaltic tephra. Minor lacustrine sediments are evident in lenticular clay layers containing rare freshwater gastropods (Hanson, 1998). Field data suggest that the volcanic rocks of the Kool Spring formation were locally derived. Air-fall deposits containing pumice lapilli with diameters of ~30–50 mm appear to represent proximal pyroclastic facies derived from Plinian-type eruptions. We have not yet been successful, however, in correlating these pumice lapilli chemically with any of the rhyolitic centers in the map area (Fig. 3C). Local sources for the interbedded Venator Ranch lavas and basalt tephra, on the other hand, are evident from north-trending Venator Ranch dikes that cut across several rock types, including the Oligocene–Miocene dacites (Fig. 5), Steens basalt, and pyroclastic rocks in the lower part of the Kool Spring formation.

#### ***Dinner Creek Tuff and Hunter Creek Basalt***

The bimodal character of flood-basalt volcanism became more prevalent in the later stages of eruption. In the south and central part of the map area, this evolution is reflected in the felsic and mafic members of the Kool Spring formation. In the northern part of the map area, it is reflected in the Dinner Creek

tuff, which is interbedded within a tholeiitic succession of chemically identical lava flows composing Birch Creek basalt below and Hunter Creek basalt above. The Birch Creek and Hunter Creek lavas are chemically indistinguishable from the Grande Ronde Basalt Formation of the Columbia River Basalt Group (Binger, 1997). Although they lie along the Steens basalt–basalt of Malheur Gorge TiO<sub>2</sub> vs. P<sub>2</sub>O<sub>5</sub> trend, the Birch Creek and Hunter Creek basalts differ from the Steens and Pole Creek (basalt of Malheur Gorge) lavas in that they are aphyric and chemically more evolved.

The Dinner Creek tuff (Greene et al., 1972) is a densely welded ignimbrite that may have erupted from a caldera near the vicinity of Castle Rock and/or Westfall Butte, ~30 km north of the map area (Rytuba and Vander Meulen, 1991; Evans and Binger, 1997). This location is consistent with the overall distribution and thinning of the Dinner Creek tuff from the Castle Rock area southward into the map area (Johnson et al., 1998b). Although it forms a spectacular marker bed throughout the Juntura Quadrangle (Fig. 8), it exists only in scattered outcrops farther to the south (Fig. 7). One such exposure overlies the Kool Spring formation in the northeast corner of the Circle Bar Quadrangle (Fig. 2).

The Dinner Creek tuff is overlain by the Hunter Creek basalt throughout the Juntura Quadrangle (Fig. 8). Its only presence beyond the Juntura region is in a small outcrop located along the western border of the Winnemucca Creek Quadrangle (Figs. 2 and 7). North-trending Hunter Creek dikes have been identified along the western border of the Oregon-Idaho graben, ~25 km east of Juntura (Cummings et al., 2000). Scattered flows of Birch Creek chemistry have been identified throughout the map area, at the top of tholeiitic sections where Dinner Creek tuff is missing. Chemically, these flows could be interpreted as Hunter Creek basalt; however, they do not display the classic hackly entablature of the Hunter Creek outcrops found elsewhere. At least one flow of Birch Creek chemistry is interbedded with Steens basalt south of the map area in the Summit Springs section (Fig. 1).

The incorporation of tachylytic lenses of Hunter Creek basalt chemistry within the Dinner Creek tuff led Evans (1990) and Evans and Binger (1998) to suggest that these two magmas may have erupted simultaneously. Both eruptions appear to have been contemporaneous, or nearly contemporaneous, with a variety of felsic eruptions from vents lying near the source area for Hunter Creek basalt,

along the western margin of the Oregon-Idaho graben, during the initial opening of the graben at ca. 15.3 Ma (Lees, 1994; Cummings et al., 2000; Hooper et al., 2002a).

#### **Early Diktytaxitic Olivine Basalts**

Small-volume diktytaxitic olivine basalt flows unconformably overlie the Hunter Creek basalt in the central and eastern parts of the Juntura Quadrangle (Fig. 8), but they are absent farther south (Fig. 7). These primitive basalt flows correspond stratigraphically with the Tims Peak basalt, originally defined by Kittleman et al. (1965) as a single flow. Binger (1997), however, demonstrated that the Tims Peak basalt can be subdivided into at least four similar, but chemically distinct flow types. Two of these chemical types, the Juniper Gulch and Grasshopper Flat basalts, are ubiquitous in the Stemler Ridge Quadrangle, immediately north of the map area (Johnson et al., 1998b). In the Juntura Quadrangle, however, Juniper Gulch basalt is absent, and Grasshopper Flat basalt is restricted to a few outcrops along the eastern margin of the map sheet. The remaining outcrops in the center part of the Juntura Quadrangle (Figs. 7 and 8) are composed of a new Tims Peak chemical type, the Bull Canyon basalt, described more fully in the section on Chemical Correlations and Petrogenesis.

The identification of thick lake sediments containing pillows and invasive lava flows of Tims Peak basalt in the Stemler Ridge Quadrangle led Johnson et al. (1998b) to suggest that a significant amount of deformation occurred after eruption of Hunter Creek basalt at ca. 15.3 Ma, but before eruption of Tims Peak basalt at ca. 13.5 Ma. This time period corresponds with explosive caldera-collapse eruptions (ca. 15.3–14.3 Ma) and with the development of distinct subbasins (ca. 14.3–12.6 Ma) in the Oregon-Idaho graben (Cummings et al., 2000).

#### **Intermediate to Felsic Calc-Alkaline Rocks Associated with Basin and Range Extension**

Eruption of the early diktytaxitic olivine basalts at ca. 13.5 Ma appears to have marked a transition between the final stages of tholeiitic flood-basalt volcanism and the beginning stages of calc-alkaline to mildly alkaline volcanism associated with Basin and Range extension. Lees (1994) and Hooper et al. (2002a) adopted the term “Keeney sequence” to describe several successions of mildly alkaline to calc-alkaline andesitic lavas in the Oregon-

<sup>1</sup>GSA Data Repository item 2003009, major and trace element analyses of the volcanic units exposed along the middle and south forks of the Malheur River in east-central Oregon, is available on the web at <http://www.geosociety.org/pubs/ft2003.htm>. Requests may also be sent to [editing@geosociety.org](mailto:editing@geosociety.org).

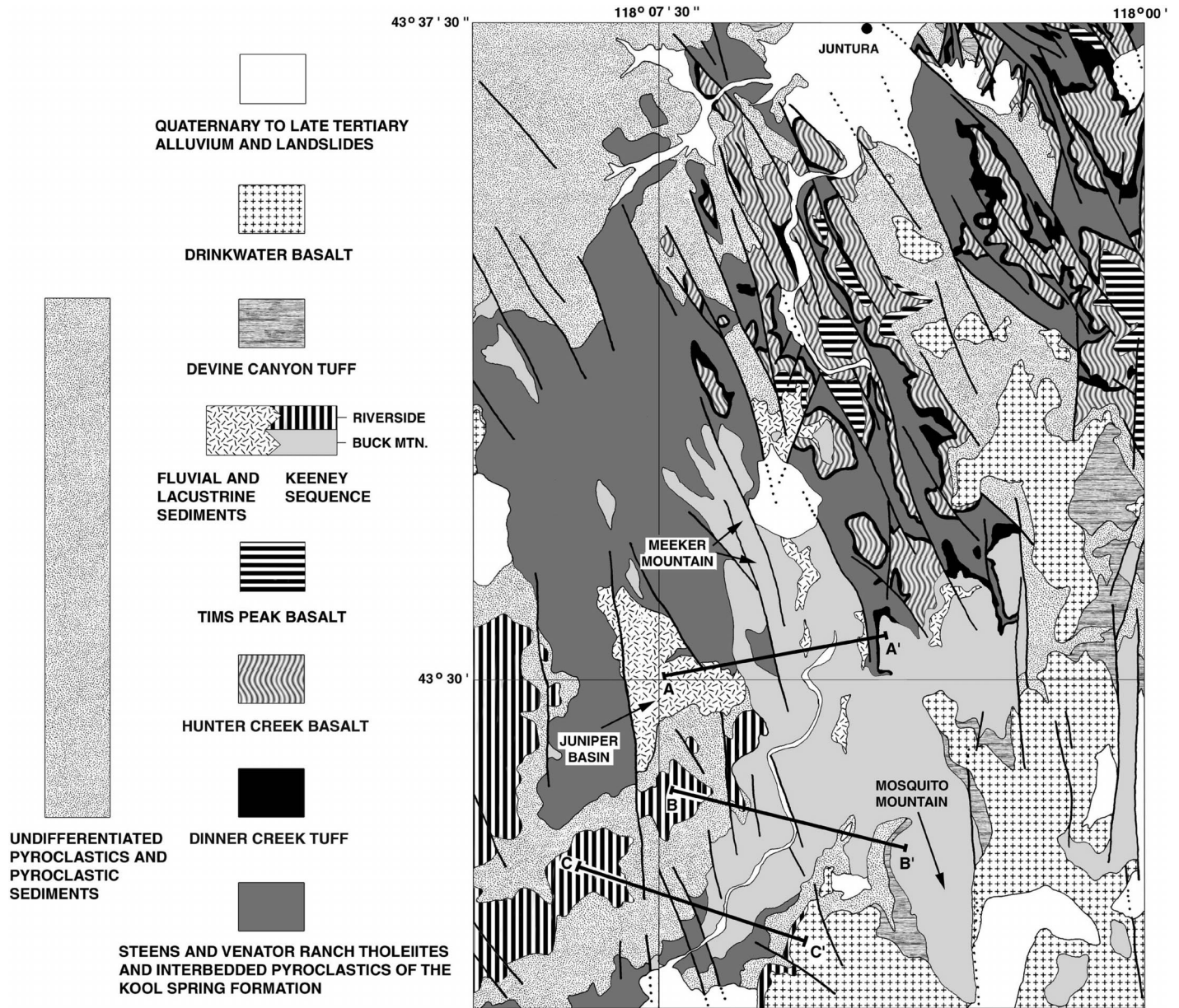


Figure 8. Simplified geologic map of the northeastern corner of the map area. Includes the Juntura Quadrangle, the eastern part of the Selle Gap Quadrangle, the northeastern corner of the Winnemucca Creek Quadrangle, and the northern part of the Mosquito Mountain Quadrangle. Cross-section locations marked as A–A', B–B', and C–C' are illustrated in Figure 9.

Idaho graben that erupted after the Tims Peak basalt, between 13.4 and 10.1 Ma. We retain this usage here, but note that the Keeney sequence is not restricted to the Oregon-Idaho graben. Rather, it is manifested in the map area by the eruption of three separate lava successions, herein referred to as the basaltic andesite of Buck Mountain, the trachyandesite of Riverside, and the basaltic trachyandesite of Cobb Creek. These Keeney sequence lavas are overlain by the Devine Canyon tuff, which was deposited across much of eastern Oregon at 9.68 Ma (Streck et al., 1999).

The trachyandesite of Riverside yielded an  $^{40}\text{Ar}/^{39}\text{Ar}$  age of  $10.14 \pm 0.23$  Ma from a sample collected from near the Warm Springs Reservoir dam (Fig. 2). The older basaltic andesite of Buck Mountain is bracketed in age by this date and the 13.5 Ma Tims Peak basalt (Fig. 4). Although chemically distinct, the Buck Mountain and Riverside flows are similar in composition to a series of Keeney sequence lavas mapped east of the map area as the Shumway Ranch basalt ( $12.4 \pm 5$  Ma, Fiebelkorn et al., 1983), the Vines Hill andesite ( $10.2 \pm 0.94$  Ma, Cummings et al., 2000), and

the Cedar Mountain andesite (Ferns et al., 1993a). The basaltic trachyandesite of Cobb Creek is tentatively considered the youngest unit of the Keeney sequence in the map area, on the basis of field evidence described in a following section.

**Basaltic Andesite of Buck Mountain**

The basaltic andesite of Buck Mountain is well exposed at its type locality in the Dunnean and McEwen Butte Quadrangles (Figs. 2 and 7), where it forms an ~300-m-thick succession of at least 15 fine-grained, generally

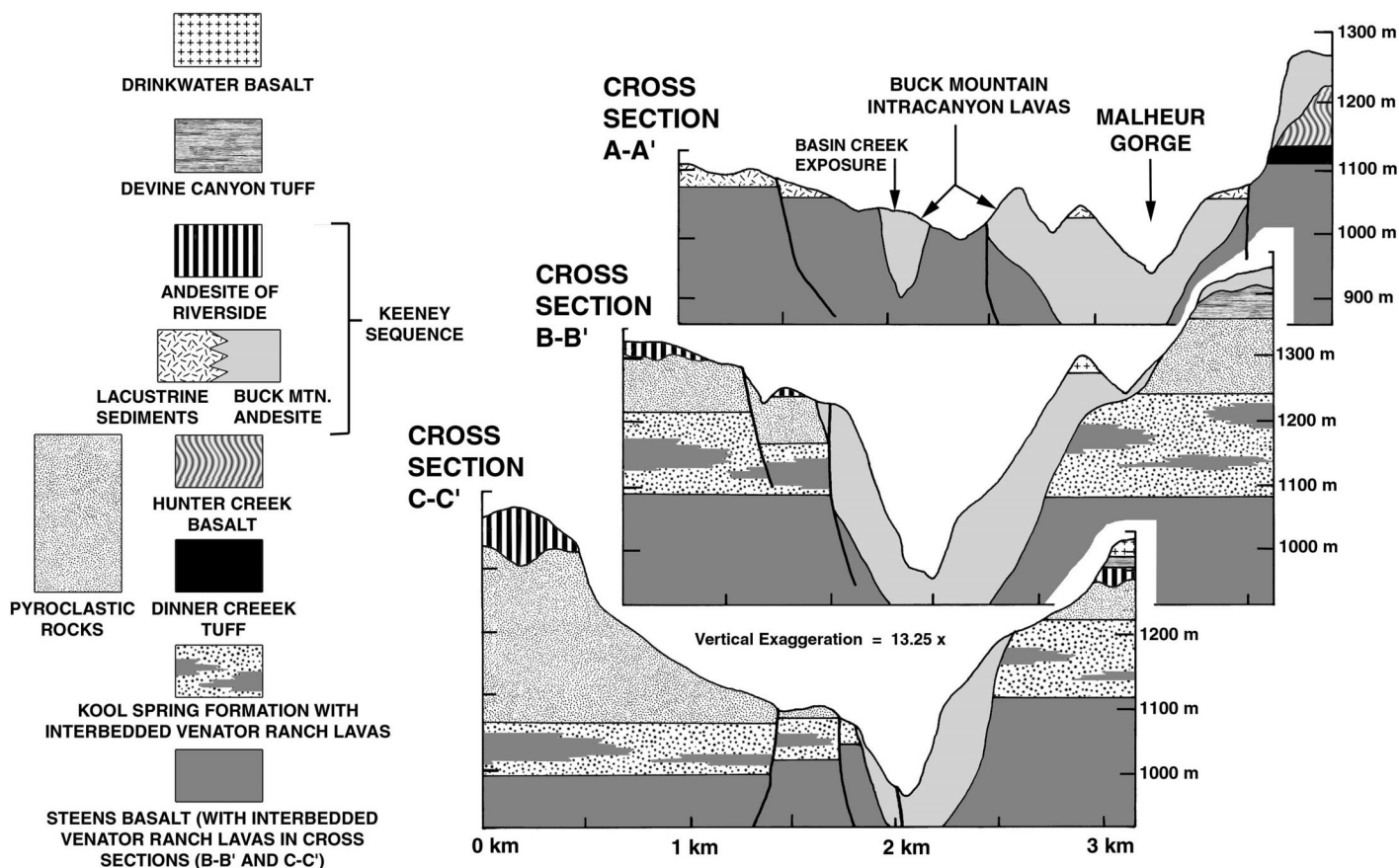


**Figure 9.** Stratigraphic cross sections across the middle fork of the Malheur River, south of Juntura and north of Riverside (for locations, see Fig. 8). The current channel of the middle fork follows the Miocene channel of the ancestral Malheur River, which was filled with Buck Mountain lava flows up to 500 m thick.

aphyric lava flows. The succession was extruded above a highly dissected erosion surface, which is best exposed ~10 km northeast of Buck Mountain, along the boundary of the Mosquito Mountain and Juntura Quadrangles (Fig. 7). Here, the local Miocene relief was well over 500 m. The lavas accumulated above an undulating plateau surface to form the high region of Meeker Mountain (1326 m) to the north and Mosquito Mountain (1533 m) to the south (Fig. 8). Between these two regions, the Buck Mountain lavas poured into deep canyons of the ancestral Malheur River and its tributaries. This thick, intracanyon succession has since been incised by the current Malheur River to a depth of ~945 m, without exposing the base of the ancestral canyon floor (Fig. 9).

Buck Mountain lavas filled these ancestral valleys in a series of closely spaced eruptions, marked by at least nine separate flows exposed in the Malheur River canyon immediately east of Meeker Mountain. Disruption of the ancestral drainage is evident in the deposition of lensoid fluvial interbeds, the thickest of which

is a 40-m-thick deposit of water-laden tuffaceous sediments and fluvial gravels of basalt and rhyolite exposed beneath a prevalent bench about halfway up the canyon wall (Fig. 10A). In places, the intracanyon stratigraphy also contains thick beds of hyaloclastite (Fig. 10B), which are particularly well exposed in Basin Creek, immediately south of Meeker Mountain (see cross section A-A', Fig. 9). Here, complete damming of the ancestral canyon disrupted the drainage beyond the confines of the canyon walls, creating a marginal lake denoted by the deposition of a thick succession of clay-rich lacustrine sediments exposed throughout the Juniper Basin, immediately west of the intracanyon exposure (Fig. 8).

#### *Trachyandesite of Riverside*

The trachyandesite of Riverside lies unconformably above the basaltic andesite of Buck Mountain in the northeastern part of the Mosquito Mountain Quadrangle (Fig. 8). It thickens to the southwest, into the Winnemucca Creek Quadrangle (Figs. 2 and 7), where it

forms a series of spectacular intracanyon outcrops up to 300 m deep (Fig. 11). Unlike the pulsate accumulation of distinct flows in the intracanyon Buck Mountain sequence (Fig. 10), the Riverside lavas largely filled these ancient canyons in a single eruptive phase, marked by the rapid accumulation of flows that typically appear to have crystallized as a single cooling unit. The intracanyon outcrops form distinct monoliths with variable jointing characteristics. Most are dominated by thick, curvi-columnar to hackly entablatures with little evidence of laterally continuous flow units (Fig. 11C); however, others are dominated by a few discontinuous flow-unit boundaries delineated by stacked successions of massive colonnades, up to 60 m high, with little evidence of intraflow entablatures (Fig. 11B). In hand specimen, the trachyandesite of Riverside is fine- to medium-grained and sparsely plagioclase-phyric (<5 mm long); it contains rare crustal xenoliths (Hanson, 1998).

#### *Basaltic Trachyandesite of Cobb Creek*

The basaltic trachyandesite of Cobb Creek comprises a single lava flow exposed in three

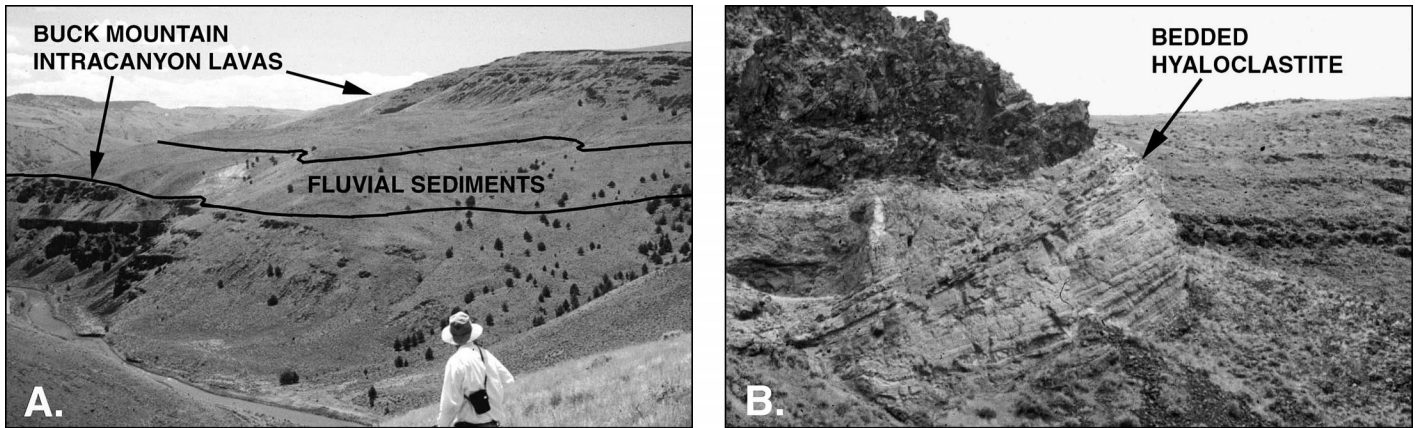


Figure 10. Buck Mountain intracanyon lavas with interbedded sediments and hyaloclastite. (A) Buck Mountain intracanyon lava flows exposed along the eastern flank of Meeker Mountain (top) and along the western canyon wall of the middle fork of the Malheur River (bottom), ~13 km south of Juntura. Distinct lava flows are separated by lensoid sedimentary interbeds, generated by the periodic disruption of the ancestral Malheur River. The thickest of these deposits is a 40-m-thick deposit of water-laden tuffaceous sediments and fluvial gravels exposed on the bench separating the upper and lower lava successions. (B) Reworked, bedded hyaloclastite deposit separating two intracanyon Buck Mountain lava flows filling a steep-walled ancestral valley, well exposed in Basin Canyon (see cross section A–A', Fig. 9).

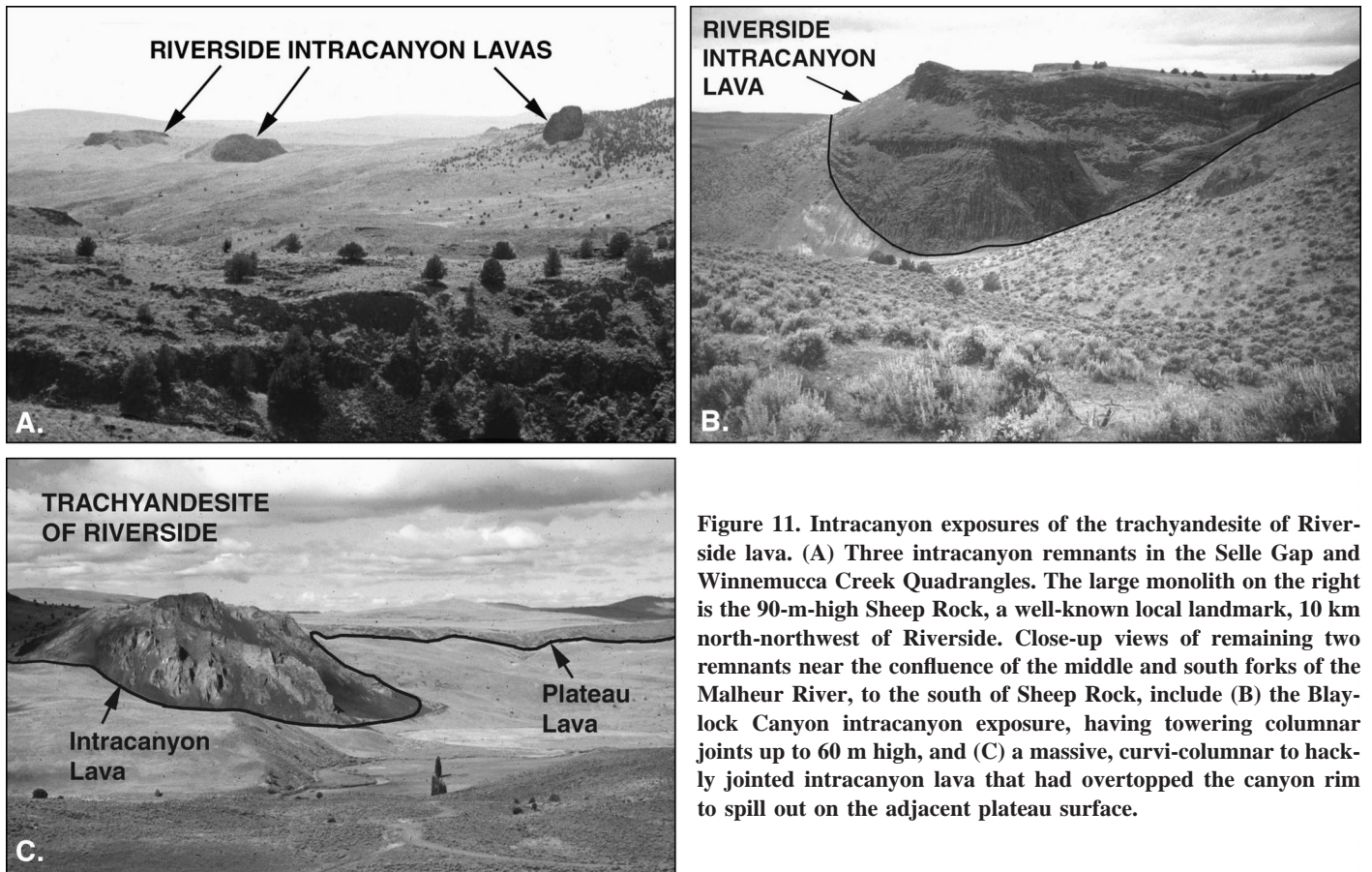


Figure 11. Intracanyon exposures of the trachyandesite of Riverside lava. (A) Three intracanyon remnants in the Selle Gap and Winnemucca Creek Quadrangles. The large monolith on the right is the 90-m-high Sheep Rock, a well-known local landmark, 10 km north-northwest of Riverside. Close-up views of remaining two remnants near the confluence of the middle and south forks of the Malheur River, to the south of Sheep Rock, include (B) the Blaylock Canyon intracanyon exposure, having towering columnar joints up to 60 m high, and (C) a massive, curvi-columnar to hackly jointed intracanyon lava that had overtopped the canyon rim to spill out on the adjacent plateau surface.

separate outcrops in the McEwen Butte Quadrangle and in smaller outcrops in the southern Winnemucca Creek Quadrangle (Fig. 7). The flow is black, fine-grained, and sparsely plagioclase-phyric (>4 mm) and is distinguished by its ubiquitous hackly entablature. It covers an undulating erosion surface, typically developed above the Kool Spring formation. Its tentative age as the youngest member of the Keeney sequence in the map area is based on its apparent deflection around an erosional remnant of the trachyandesite of Riverside in the northeastern corner of the McEwen Butte Quadrangle.

#### *Devine Canyon Tuff*

The ca. 9.68 Ma Devine Canyon tuff (Streck et al., 1999) forms an important stratigraphic marker throughout southeastern Oregon. After erupting from near Burns, in the Harney Basin (Fig. 1), this greenish-gray crystal-rich ignimbrite spread eastward into the Oregon-Idaho graben (Walker, 1979; Binger, 1997; Cummings et al., 2000). In the map area between these two regions, the Devine Canyon tuff forms extensive outcrops in the southern quadrangles, but only scattered outcrops to the north (Fig. 7). Farther south, at least one exposure of the Devine Canyon tuff appears to thin around the faulted base of the Steens Mountain uplift at Summit Springs (Fig. 1; mapping by Camp and Ross). This overall outcrop pattern is consistent with the eastward advance of the pyroclastic sheet flow through a northwest-trending topographic low, partly extending across the southern map area and that region lying north of the Steens Mountain uplift. Such a corridor is consistent with the interpretation of Johnson (1995) that most of the uplift on the Steens Mountain fault occurred between 12 and 10 Ma.

#### **Late Diktytaxitic Olivine Basalts**

The Devine Canyon tuff is unconformably overlain by a series of medium-gray, diktytaxitic lava flows, which in hand specimen resemble the older diktytaxitic olivine-bearing Tims Peak basalt. As a group, however, these younger basalts correspond in time with the eruption of late Miocene–Holocene, high-alumina olivine tholeiite (HAOT), which forms the youngest lava flows across much of the northern Basin and Range province (Hart et al., 1984). In the map area, these mafic lavas are subdivided into two age groups: the late Miocene Drinkwater basalt and the late Pleistocene Voltage flow.

#### *Drinkwater Basalt*

Several gently tilted and moderately deformed mesas in the map area are capped by a succession of lava flows, collectively named the Drinkwater basalt (Shotwell, 1963). Some of these mesas are locally capped by a single lava flow, but more typically by two or more flows that can reach cumulative thicknesses of up to 70 m. The northern outcrops of Drinkwater basalt appear to be confined to a northwest-trending structural depression that also incorporates late Miocene–Pliocene tuffaceous sediments of the Juntura Basin (Figs. 3B and 7).

Petrographically, the Drinkwater lava flows vary from diktytaxitic to subophitic, with common microphenocrysts of olivine, together with phenocrysts and/or glomerocrysts of plagioclase. One mesa-forming Drinkwater basalt flow, located ~2 km northwest of the Circle Bar Quadrangle (Fig. 2), yielded a K-Ar age of  $6.91 \pm 1.09$  Ma (Greene et al., 1972).

#### *Voltage Flow*

This late Pleistocene lava flow appears to have erupted from several vents located north of Diamond Craters, ~25 km southwest of the map area (Greene et al., 1972). The flow advanced into the south fork of the Malheur River canyon, extending northward through the map area to its terminus in the southern Juntura Quadrangle (Fig. 7). This exceptional flow traveled >50 km, fed by at least one lava tube exposed at Malheur Cave near the southern boundary of the map area. Near its source in the Harney Basin (Fig. 1), the Voltage flow forms a high-standing subdued ridge marking the eastern boundary of pluvial Lake Malheur (Walker and Swanson, 1968). Radiocarbon dating of mollusk shells found in the oldest beach terrace of this pluvial lake led Gehr and Newman (1978) to suggest that the age of the Voltage flow is >32,000 yr B.P.

### **CHEMICAL CORRELATIONS AND PETROGENESIS**

The sampling program generated 282 samples that were chipped and carefully handpicked to yield the freshest material. Each sample was analyzed by XRF (X-ray fluorescence) for major elements and 17 trace elements (Ni, Cr, Sc, V, Ba, Rb, Sr, Zr, Y, Nb, Ga, Cu, Zn, Pb, La, Ce, and Th). Representative samples of each geologic unit were further analyzed by inductively coupled plasma source mass spectrometry (ICP-MS) for the 14 rare earth elements, together with Ba, Rb, Y, Nb, Cs, Hf, Ta, Pb, Th, U, and Sr. The complete data set in-

cludes 130 analyses of the lower tholeiitic rock types, 70 analyses of the overlying calc-alkaline to mildly alkaline rock types, 24 analyses of the lower and upper diktytaxitic olivine basalts, and 58 analyses of the felsic rock types. A representative data set of XRF and ICP-MS analyses of each map unit is presented in Tables 1 and 2. The complete data set is available in the Data Repository (see text footnote 1).

#### **The Basaltic Rocks**

##### *Steens, Basalt of Malheur Gorge, and Hunter Creek Basalts*

The total alkali vs. silica (TAS) diagram of LeBas et al. (1986) (Fig. 12) helps to illustrate lateral chemical variations in the tholeiitic succession, from Steens basalt collected at Steens Mountain south of the map area (Johnson et al., 1998a) to the basalt of Malheur Gorge collected northeast of the map area (Binger, 1997). The two shaded fields in Figure 12A represent lavas collected in the lower one-third and upper two-thirds of the Steens Mountain section; the stratigraphic boundary occurs near the base of the geomagnetic polarity transition delineated by Mankinen et al. (1987). Lower Pole Creek analyses (basalt of Malheur Gorge) fall within the lower Steens basalt field (Fig. 12B), consistent with Binger's (1997) interpretation that these basalt types are chemically equivalent and laterally continuous. Such lateral continuity is lacking for the upper Pole Creek and Birch Creek lavas, which are absent in the Steens Mountain section (Fig. 12B), and for the upper Steens basalt, which is absent northeast of the map area. However, the undifferentiated Steens basalt–basalt of Malheur Gorge lavas within the map area (Fig. 12C) fall across all field boundaries, thus marking a transition zone of northward-diminishing upper Steens basalt eruptions and northward-increasing upper Pole Creek and Birch Creek eruptions.

As defined in their type areas, the lower and upper Pole Creek basalt flows, and the lower and upper Steens basalt flows, display clear, upward-progressive chemical variations in the basalt stratigraphy (Gunn and Watkins, 1970; Binger, 1997). It is important to emphasize, however, that these chemical subtypes can not be used as strict stratigraphic markers. Lavas of each subtype can be found interbedded with one another, even in their type areas (Binger, 1997; Johnson et al., 1998a). These interbedded relationships become even more apparent in the present map area, where each chemical type to the north and south can be found interbedded in stratigraphic sections, typically

TABLE 1. SELECTED ANALYSES OF MAFIC AND INTERMEDIATE ROCK TYPES

Rock unit	Undifferentiated Steens–Malheur Gorge				Venator Ranch				Grasshopper Flat	Bull Canyon	Buck Mountain		Riverside		Cobb Creek	Drinkwater	Votage
	CR7–11	CR7–125	CR7–26	CR7–128	CR7–20	CR7–79	CR7–138	BH6–25	CR9–251	CR9–269	HC6–1	HC6–6	BH6–15	BH6–18	CR8–139	CR8–135	BH6–5
SiO <sub>2</sub>	49.73	52.7	52.09	48.31	49.99	47.7	47.55	50.14	49.35	52.87	56.37	60.46	58.11	58.64	53.18	50.95	47.13
Al <sub>2</sub> O <sub>3</sub>	17.49	14.54	14.5	15.48	16.09	15.17	14.94	14.31	16.72	16.46	16.9	16.93	17.67	17.09	15.76	16.56	16.6
TiO <sub>2</sub>	2.18	2.53	2.6	3.1	1.79	2.17	2.71	2.7	0.94	0.71	1.1	0.98	1	0.98	2.15	1.35	0.88
FeO	10.29	12.78	12.78	13.32	10.62	12.47	12.53	12.5	9.66	7.98	7.32	6.01	6.67	6.23	9.99	9.38	9.21
MnO	0.12	0.19	0.2	0.19	0.18	0.2	0.21	0.16	0.17	0.17	0.1	0.09	0.12	0.12	0.17	0.17	0.16
CaO	9.19	6.77	7.18	8.43	9.73	9.2	9.82	8.37	11.03	9.63	6.89	5.82	6.41	5.89	7.01	9.58	10.98
MgO	4.63	4.17	4.33	5.28	6.24	7.85	6.36	5.11	7.94	8.17	3.72	2.68	2.79	2.97	3.5	7.24	9.7
K <sub>2</sub> O	0.68	1.71	1.72	1.13	0.88	0.82	0.95	1.25	0.35	0.89	1.85	2.33	1.83	2.41	2.09	1.14	0.25
Na <sub>2</sub> O	3.16	3.64	3.49	3.33	2.89	2.77	2.82	2.74	2.36	2.48	4.16	4.48	4.66	4.07	3.64	2.83	2.68
P <sub>2</sub> O <sub>5</sub>	0.29	0.43	0.43	0.64	0.44	0.61	0.8	0.69	0.18	0.14	0.43	0.35	0.48	0.46	0.85	0.33	0.12
XRF trace elements																	
Ni	78	57	49	98	90	123	53	58	182	135	34	31	22	22	9	115	187
Cr	77	59	67	103	75	188	164	140	312	285	54	26	30	33	12	168	354
V	248	276	301	291	253	263	624	286	225	181	165	152	148	141	226	208	214
Zr	161	210	208	260	130	156	186	233	59	70	197	199	170	172	260	136	66
Ga	23	22	23	23	22	18	24	20	17	16	17	19	21	21	21	17	19
Cu	67	120	71	180	43	51	39	36	126	103	45	36	40	48	25	57	77
Zn	92	127	127	133	90	109	126	127	73	59	86	74	77	83	119	76	66
ICP-MS trace elements																	
Ba	329	436	439	441	360	566	620	728	462	349	837	974	806	919	1145	533	110
Th	1.98	3.53	3.33	3.11	2.1	1.23	1.24	2.08	0.56	1.8	2.29	2.87	1.78	1.44	2.85	0.97	0.28
Nb	11.53	17.01	17.14	22.85	15.9	14.85	19.98	20.5	3.79	3.61	13	11.65	15.68	11.38	19.23	7.56	2.94
Y	31.37	38.76	39.39	45.12	31.78	35.48	41.68	42.97	24.31	22.68	25.99	25.23	23.06	22.21	10.04	31.27	18.76
Hf	4.28	5.85	5.89	6.96	3.3	3.74	4.59	5.61	1.56	1.98	4.59	4.84	3.91	3.87	6.31	3.46	1.52
Ta	0.8	1.21	1.18	1.46	3.25	3	2.83	1.23	0.22	0.26	0.76	0.7	0.89	0.63	1.17	1.95	0.19
U	0.74	1.42	1.36	1.12	0.64	0.3	0.35	0.74	0.22	0.74	0.8	1.05	0.71	0.67	0.93	0.28	0.1
Pb	3.82	7.79	7.52	5.24	3.93	3.33	3.59	6.66	2.65	4.75	7.62	9.1	6.14	9.01	10	3.07	0.82
Rb	11.3	3.97	10.3	24	14.4	10.9	11.5	20.7	5	17.7	28.4	43.6	22.6	21.6	35	16.2	3.2
Cs	0.53	1.47	1.49	0.73	0.17	0.12	0.18	0.33	0.21	0.87	0.3	0.91	0.41	0.36	0.61	0.17	0.04
Sr	450	391	431	460	311	319	375	366	303	235	573	522	718	709	493	291	209
Sc	27.4	28.2	30.8	29.6	30.9	32.3	37.1	30.3	39.3	36.3	21.1	17.8	16.17	16.2	25	32.4	36.1
La	15.91	26.3	25.99	29.95	17.78	20.82	26.15	32.34	8.84	8.64	29.2	28.82	26.1	25.47	40.97	16.08	4.46
Ce	33.36	55.37	56.2	65.4	35.82	43.22	54.34	66.21	13.86	17.24	55.52	52.9	51.05	49.86	78.65	29.51	9.92
Pr	4.57	6.93	7.03	8.34	4.58	5.63	7.13	8.31	2.08	2.16	6.41	6.35	6.02	6.04	9.39	4.09	1.5
Nd	21.27	30.67	31.97	38.13	20.55	25.91	31.67	36.91	9.85	9.64	26.27	25.15	24.08	24.86	39.83	18.3	7.06
Sm	5.86	8.56	8.62	10.33	5.28	6.56	8.42	8.83	2.81	2.77	5.58	5.2	5.04	5.06	9.11	4.9	2.28
Eu	1.97	2.29	2.41	2.96	1.81	2.33	2.95	2.85	1.04	0.85	1.65	1.48	1.5	1.54	2.79	1.69	0.96
Gd	6.2	8.27	8.24	9.77	5.41	6.74	8.38	8.75	3.34	3.2	5.14	5.01	4.54	4.51	8.36	5.37	2.89
Tb	0.99	1.31	1.32	1.59	0.91	1.1	1.34	1.39	0.59	0.58	0.81	0.76	0.7	0.68	1.29	0.91	0.52
Dy	5.84	7.74	7.94	9.34	5.66	6.44	7.83	8.18	3.86	3.87	4.79	4.67	4.11	3.94	7.62	5.75	3.41
Ho	1.19	1.52	1.53	1.78	1.19	1.34	1.61	1.6	0.82	0.84	0.96	0.93	0.8	0.77	1.5	1.17	0.72
Er	3.02	3.93	4	4.44	3.15	3.55	4.16	4.2	2.28	2.47	2.63	2.42	2.15	2.11	3.95	3.18	2.04
Tm	0.42	0.56	0.56	0.62	0.45	0.49	0.59	0.6	0.33	0.36	0.38	0.37	0.32	0.31	0.56	0.46	0.31
Yb	2.45	3.43	3.36	3.67	2.89	3.06	3.6	3.64	2.08	2.31	2.34	2.31	2.08	1.99	3.47	2.87	1.9
Lu	0.39	0.52	0.51	0.55	0.55	0.55	0.55	0.55	0.37	0.37	0.37	0.37	0.33	0.33	0.54	0.45	0.29

Note: The complete geochemical data set of major and trace elements may be obtained free from the GSA Data Repository. XRF—X-ray fluorescence, ICP-MS—inductively coupled plasma mass spectroscopy.

without any clear upward progression of chemical change.

As a group, the Steens and basalt of Malheur Gorge lavas have relatively low Mg numbers [Mg# = 100 × MgO/(MgO + FeO)] moderate to high SiO<sub>2</sub> contents, and low Ni contents, all of which suggest that they are not primary magmas, but rather differentiated magmas modified by gabbroic fractionation. Such a process is indicated by major and trace element analyses that appear to define broadly linear crystallization trends progressing from the most primitive basalt of lower Steens (lower Pole Creek) to the upper Pole Creek basalt, to the more evolved Birch Creek and Hunter Creek basaltic andesite. It seems clear that these basaltic groups are closely related to one another by similar fractional-crystallization

processes. However, it is just as clear that fractional crystallization was not the sole mechanism in their genesis, as indicated by the spread of analyses along the crystallization trends. The overall broadness of these trends may be related to the crystallization of diverse primary magmas derived from variable degrees of partial melting or to crystallization accompanied by crustal assimilation (AFC—assimilation and fractional crystallization) and/or magma recharge. Such open-system processes are consistent with the conclusions of Hart et al. (1989) for Steens-type tholeiitic lavas farther south. However, we cannot entirely rule out the possible contributions of more superficial factors such as analytical imprecision and variations in phenocryst volume.

Derivation of the upper Steens basalt flows,

however, requires a more complex scenario. Upper Steens basalt flows display consistently higher concentrations of incompatible elements (e.g., Ti, Zr, P, K, Sr, Rb, Ba) when compared to lower Steens (lower Pole Creek) lavas having identical indices of fractionation (e.g., Mg#). Thus, the upper Steens basalt flows cannot have been derived via simple fractional crystallization of lower Steens basalt magmas.

The TAS diagram (Fig. 12A) demonstrates that most flows of the upper Steens basalt at Steens Mountain are not classic tholeiites, but rather mildly alkaline basalts and trachybasalts, lying above the alkali-subalkali field boundary of Irvine and Baragar (1971). Their alkalic character appears to decrease northward into the map area (Fig. 12C) and beyond

TABLE 2. SELECTED ANALYSES OF FELSIC ROCK TYPES

Rock unit	Swamp Creek		Circle Bar		Devine Canyon	Dinner Creek	Black Butte	McEwen Butte	Visher Creek
Sample	CR7-103	CR8-191	CR7-64	CR7-71	CR7-4	CR9-240	CR9-245	CR8-152	CR8-189
SiO <sub>2</sub>	75.64	73.49	74.58	76.06	74.22	77.55	77.06	72.05	77.38
Al <sub>2</sub> O <sub>3</sub>	14.14	14.03	13.14	13.17	10.99	11.7	12.7	13.16	11.18
TiO <sub>2</sub>	0.06	0.06	0.16	0.07	0.23	0.16	0.13	0.28	0.07
FeO	0.99	1.01	1.2	0.71	2.82	1.82	1.07	2.02	1.07
MnO	0.08	0.03	0.05	0.05	0.04	0.04	0	0.04	0.01
CaO	1.22	1.1	1.12	0.88	0.7	0.33	0.15	1.12	0.3
MgO	0.2	0	0.65	0.34	0.33	0	0	0.27	0
K <sub>2</sub> O	4.43	4.59	5.5	5.31	5.84	3.73	4.72	6.16	4.71
Na <sub>2</sub> O	4.02	3.63	3.14	3.11	2.97	4.26	3.98	2.65	3.03
P <sub>2</sub> O <sub>5</sub>	0.03	0.03	0.06	0.03	0.04	0.02	0.02	0.07	0.03
XRF trace elements									
Ni	7	12	7	10	14	7	8	8	12
Cr	0	0	0	0	0	0	1	2	0
V	10	2	20	6	12	9	0	17	0
Zr	79	77	109	78	976	390	297	209	141
Ga	16	15	16	16	30	20	23	17	19
Cu	7	18	7	5	6	1	3	10	11
Zn	42	28	26	20	225	111	89	39	53
ICP-MS trace elements									
Ba	844	897	447	149	70	1398	22	806	14
Th	4.08	4.54	14.81	15.86	11.08	7.77	15.16	12.03	14.22
Nb	12.48	10.79	13.49	13.16	80.41	23.81	55.45	16.05	36.37
Y	27.08	19.99	23.78	22.01		76.49	57.8	35.87	51.64
Hf	3.2	3.18	3.83	3.24	23.47	11.05	10.78	6.63	6.47
Ta	0.93	2.21	1.71	1.96	4.93	1.46	3.76	2.9	3.99
U	2.39	1.8	7.47	9.64	4.76	3	4.79	4.38	3.87
Pb	18.59	18.34	21.83	25.69	29.23	15.37	23.67	17.77	23.15
Rb	96.5	95.9	167.1	187.2	130.9	71	161.4	143.8	150.8
Cs	2.92	2.12	7.27	9.85	4.12	1.9	2.58	3.36	1.81
Sr	130	126	110	61	30	28	7	87	6
Sc	4.1	3.4	3.2	2.2	2	4.5	0.8	4	0.8
La	16.04	19.75	25.83	15.84	88.42	38.24	54.43	40.98	43.24
Ce	28.8	28.42	43.63	29.1		80.4	84.36	74.22	82.11
Pr	3.27	4.2	4.6	3.17	19.76	9.19	12.62	8.01	9.62
Nd	13.06	16.73	17.18	11.98	80.66	37.5	47.29	30.16	37.01
Sm	3.59	4.03	3.77	3.1	21.14	9.58	11.88	6.55	9.44
Eu	0.54	0.66	0.56	0.35	0.78	1.5	0.29	0.83	0.15
Gd	3.75	3.78	3.33	2.95	21.35	9.79	10.4	5.77	8.35
Tb	0.68	0.64	0.57	0.55	3.79	1.89	1.9	0.98	1.56
Dy	4.28	3.66	3.53	3.42	24.28	12.9	11.83	6.02	9.7
Ho	0.89	0.69	0.75	0.71	5.21	2.85	2.3	1.28	2
Er	2.43	1.76	2.16	2.06	14.25	8.37	6.5	3.64	5.4
Tm	0.37	0.26	0.35	0.33	2.16	1.33	0.99	0.58	0.82
Yb	2.47	1.57	2.34	2.28	13.8	8.82	6.28	3.83	5.02
Lu	0.4	0.23	0.4	0.38	2.28	1.43	0.92	0.6	0.74

Note: The complete geochemical data set of major and trace elements may be obtained free from the GSA Data Repository. XRF—X-ray fluorescence, ICP-MS—inductively coupled plasma mass spectroscopy.

it to the northeast (Fig. 12B). Experimental data show that transitional to mildly alkaline magmas, similar to upper Steens basalt, can be generated by small degrees of partial melting, at greater depths of melting than tholeiitic magmas with equivalent silica contents (Green and Ringwood, 1967; Hirose and Kushiro, 1993). This progression is typical of many large-volume basaltic shield volcanoes and lava fields in both continental and oceanic environments. Two examples include the tholeiitic and younger alkalic stages inherent in the haratt lavas of western Saudi Arabia (Camp and Roobol, 1992) and in the shield volcanoes of Hawaii (Clague, 1987), both of which are thought to have evolved through decreasing degrees of partial melting with time.

The relatively high average K<sub>2</sub>O values for

the upper Steens lavas, however, could also be attributed to crustal contamination, a process advocated by Carlson and Hart (1987) and Hart et al. (1989) for the entire Steens basalt sequence. Crustal assimilation should be reflected in higher concentrations of large ion lithophile elements (LILEs) with respect to the high field strength elements (HFSEs), because the latter are not as easily liberated from crustal sources. Indeed, the upper Steens lavas appear to have higher LILE/HFSE ratios (e.g., Ba/Zr) than lower Steens lavas. A very high degree of crustal assimilation, however, would be required to produce the elevated LILE (K, Ba, Rb, Sr) values for upper Steens basalt, which on average are about twice those for lower Steens basalt having equivalent Mg numbers and SiO<sub>2</sub> contents.

Because crustal contamination has little effect on TiO<sub>2</sub>/P<sub>2</sub>O<sub>5</sub> ratios, any variation in this ratio should reflect bulk compositional variations in the mantle source (Carlson and Hart, 1988). The lower and upper parts of the Steens basalt display two parallel, but distinct TiO<sub>2</sub> vs. P<sub>2</sub>O<sub>5</sub> trends (Fig. 13B), suggesting that they may have been derived from similar but slightly different sources. Although Steens basalt may well have been modified by crustal contamination (Hart et al., 1989), the extent of this process remains inconclusive. The progressive upward change in incompatible element ratios (e.g., Ba/Zr, TiO<sub>2</sub>/P<sub>2</sub>O<sub>5</sub>) from the lower to the upper Steens basalt may simply denote decreasing degrees of partial melting, at greater depths of melting, tapping subtly different mantle sources with advancing time.

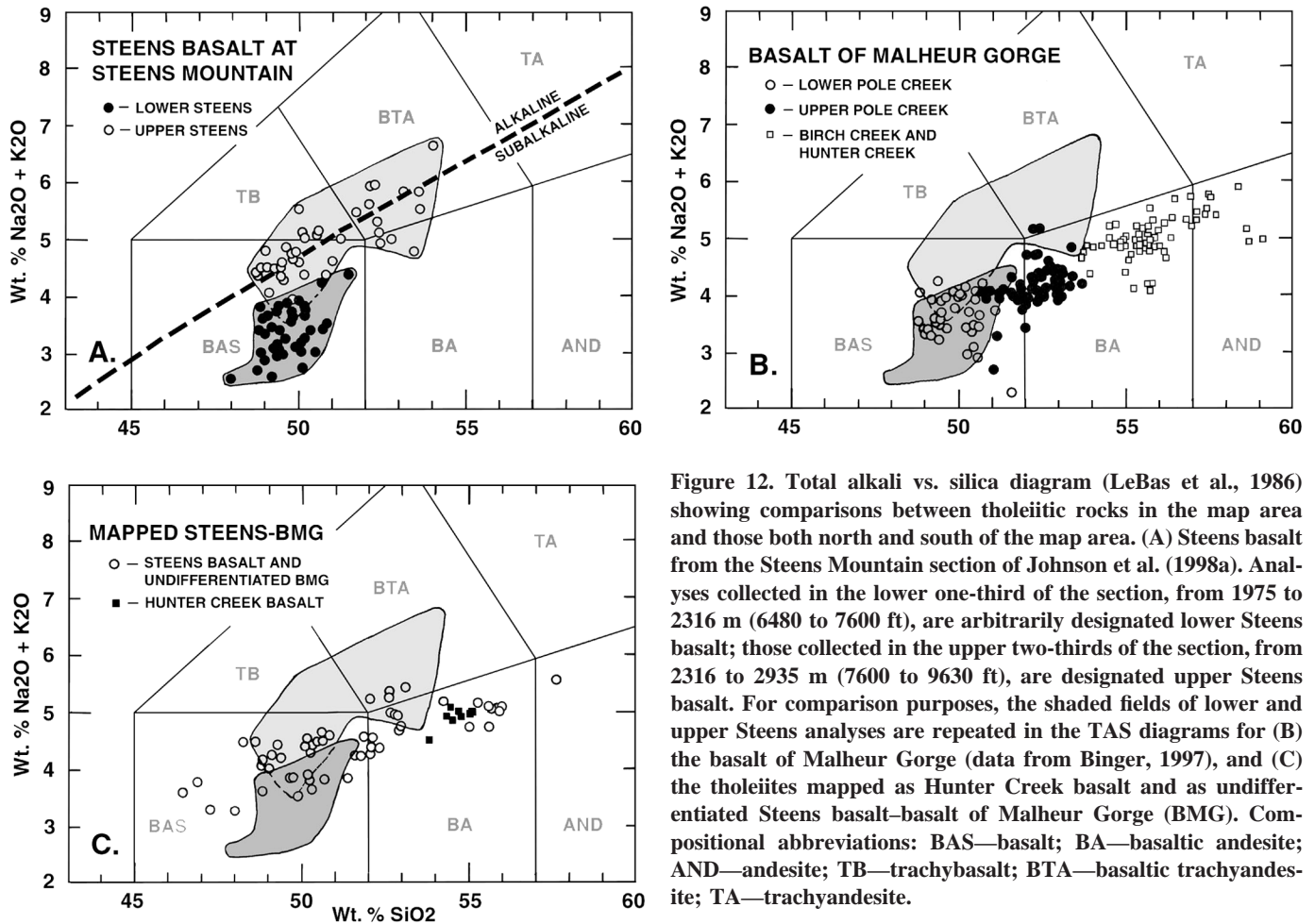


Figure 12. Total alkali vs. silica diagram (LeBas et al., 1986) showing comparisons between tholeiitic rocks in the map area and those both north and south of the map area. (A) Steens basalt from the Steens Mountain section of Johnson et al. (1998a). Analyses collected in the lower one-third of the section, from 1975 to 2316 m (6480 to 7600 ft), are arbitrarily designated lower Steens basalt; those collected in the upper two-thirds of the section, from 2316 to 2935 m (7600 to 9630 ft), are designated upper Steens basalt. For comparison purposes, the shaded fields of lower and upper Steens analyses are repeated in the TAS diagrams for (B) the basalt of Malheur Gorge (data from Binger, 1997), and (C) the tholeiites mapped as Hunter Creek basalt and as undifferentiated Steens basalt—basalt of Malheur Gorge (BMG). Compositional abbreviations: BAS—basalt; BA—basaltic andesite; AND—andesite; TB—trachybasalt; BTA—basaltic trachyandesite; TA—trachyandesite.

In contrast, the progressive compositional change (increasing  $\text{SiO}_2$  and decreasing Mg numbers) from lower Pole Creek (lower Steens) to upper Pole Creek, Birch Creek, and Hunter Creek basalts appears to be more consistent with incremental gabbroic crystallization, possibly modified by other processes.

#### Venator Ranch Basalt

The Venator Ranch basalt is chemically distinct, but with compositional similarities to both Tims Peak basalt and to the Steens basalt—basalt of Malheur Gorge—Hunter Creek sequence. Like the undifferentiated Steens basalt—basalt of Malheur Gorge lavas in the map area, the Venator Ranch basalt flows are tholeiitic lavas that vary along Fe-enrichment trends, from basalt to basaltic andesite (Fig. 14). However, the Venator Ranch lavas contain more primitive end members, and overall higher average MgO (6.39% vs. 5.01%), higher average Cr (174 ppm vs. 91 ppm), and lower average  $\text{SiO}_2$  (50.23% vs. 51.35%). Although both basalt sequences have overlapping concentrations

for most major and trace elements, the Venator Ranch basalt flows have lower average Sr values (333 ppm vs. 387 ppm) and higher average Ba values (641 ppm vs. 495 ppm). What is more important, they can be readily distinguished from the undifferentiated Steens basalt—basalt of Malheur Gorge—Hunter Creek lavas by their lower  $\text{TiO}_2/\text{P}_2\text{O}_5$  ratios (Fig. 13C). The Venator Ranch and Steens basalt—basalt of Malheur Gorge sequences appear to lie along independent paths of crystal fractionation (Figs. 15A, 15B). Their disparate  $\text{TiO}_2/\text{P}_2\text{O}_5$  ratios (Fig. 13C) suggest that they are largely composed of differentiated lavas derived from distinct mantle sources.

The most mafic end members of Venator Ranch basalt are very similar in composition to Tims Peak basalt. Both basalt types lie along similar  $\text{TiO}_2$  vs.  $\text{P}_2\text{O}_5$  trends (Figs. 13C, 13D), which suggests that they may have been derived from similar mantle sources. However, Hooper et al. (2002a) have demonstrated that the various chemical types of Tims Peak basalt fall along transitional to calc-alkaline

trends of differentiation. Although the vast majority of Venator Ranch basalt flows are tholeiitic, seven Venator Ranch lavas lie in the calc-alkaline field of Figure 14, coincident with the Tims Peak differentiation trend. However, these same analyses lie along a  $\text{P}_2\text{O}_5$  vs. Sr trend consistent with all other Venator Ranch lavas and quite distinct from the  $\text{P}_2\text{O}_5$  vs. Sr trend defined by the various chemical types of Tims Peak basalt (Fig. 16).

#### Diktytaxitic Olivine Basalts

The older (Tims Peak) and younger (Drinkwater and Voltage) diktytaxitic olivine basalts are among the most primitive of the basalt eruptions, with Mg numbers between 65 and 55 (Fig. 15). They have moderately high  $\text{Al}_2\text{O}_3$  contents (16%–17%) and similar  $\text{TiO}_2/\text{P}_2\text{O}_5$  ratios (Fig. 13D). These lavas are physically and compositionally similar to the late Miocene HAOT basalts found across much of eastern Oregon (Hart et al., 1984). As a group, they straddle the tholeiite—calc-alkaline field boundary of Figure 14, but unlike the HAOTs,

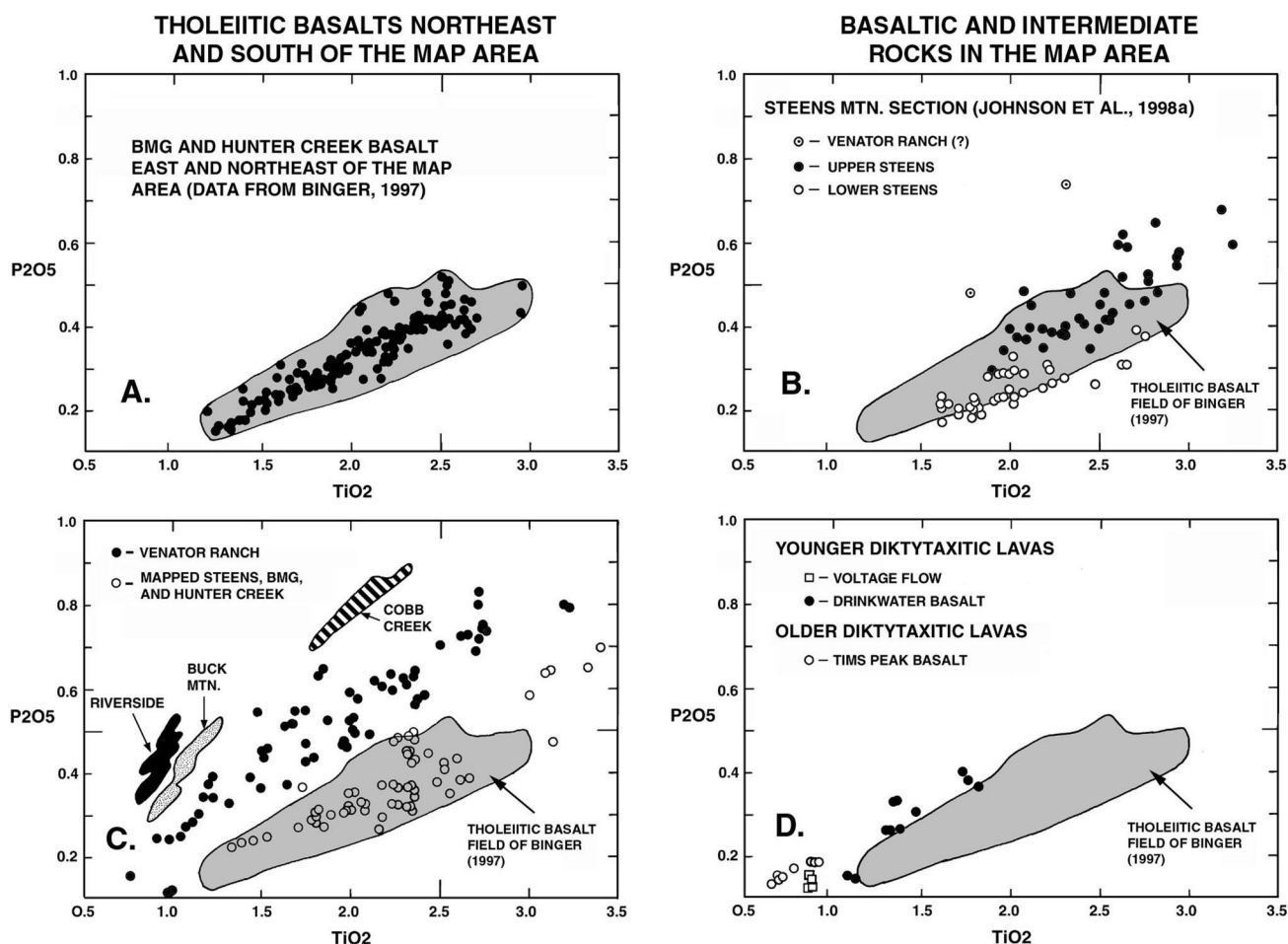


Figure 13.  $TiO_2$  vs.  $P_2O_5$  diagrams. (A) Tholeiitic basalts north and northeast of the map area (from Binger, 1997). Shaded field is repeated in each of the following diagrams. BMG—basalt of Malheur Gorge. (B) Tholeiitic basalts from the Steens Mountain section south of the map area (from Johnson et al., 1998a). (C) Mapped tholeiitic basalts (undifferentiated Steens basalt, basalt of Malheur Gorge, Venator Ranch, and Hunter Creek lavas) and intermediate-composition lavas of the Keeney sequence (Buck Mountain, Riverside, and Cobb Creek lavas). (D) Mapped diktytaxitic lavas of Tims Peak, Drinkwater, and Voltage basalts.

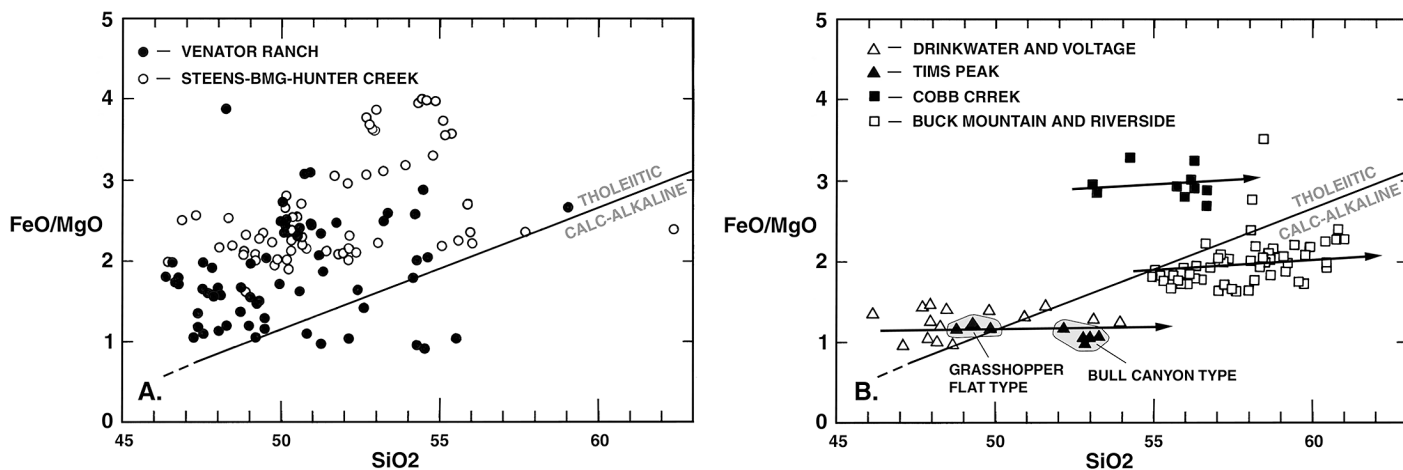


Figure 14.  $FeO/MgO$  vs.  $SiO_2$  diagram of Miyashiro (1974). (A) The Venator Ranch basalt and undifferentiated tholeiitic rocks of Steens, basalt of Malheur Gorge (BMG), and Hunter Creek. (B) Intermediate-composition rocks of the Keeney sequence (Buck Mountain, Riverside, and Cobb Creek), and the diktytaxitic Tims Peak, Drinkwater, and Voltage basalts.

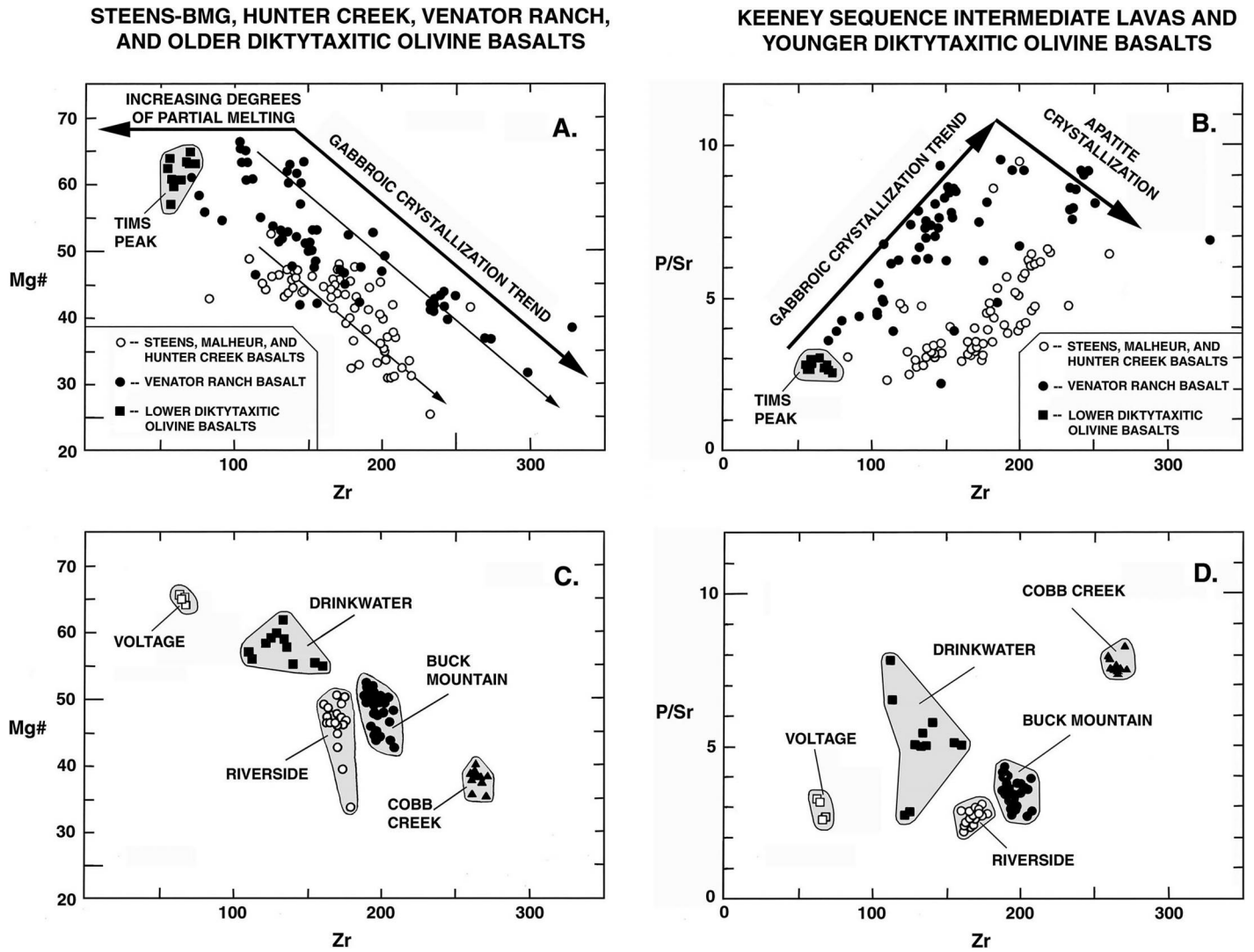


Figure 15. Zr variation diagrams for the basaltic to intermediate rock types. (A) Zr vs. Mg# for the tholeiitic rocks (Venator Ranch, undifferentiated Steens-basalt of Malheur Gorge [BMG]-Hunter Creek) and Tims Peak basalt. (B) Zr vs. P/Sr for the tholeiitic rocks (Venator Ranch, undifferentiated Steens-basalt of Malheur Gorge-Hunter Creek) and Tims Peak basalt. (C) Zr vs. Mg# for the Keeney sequence lavas (Buck Mountain, Riverside, and Cobb Creek) and the younger diktytaxitic rocks (Drinkwater and Voltage basalts). (D) Zr vs. P/Sr for the Keeney sequence lavas (Buck Mountain, Riverside, and Cobb Creek) and the younger diktytaxitic rocks (Drinkwater and Voltage basalts).

they appear to define a calc-alkaline trend of differentiation that lacks the progressive Fe enrichment expected of tholeiitic magmas.

Of the 10 Tims Peak basalt analyses in the map area, three correspond with the Grasshopper Flat chemical type of Binger (1997). The remaining seven define a new chemical type herein designated the Bull Canyon basalt. Although the Bull Canyon basalt analyses are similar to Grasshopper Flat chemistry, they are chemically distinct in that they have higher overall ranges in SiO<sub>2</sub> (52.21–53.87% vs. 48.87–49.87%) and Rb (15–19 ppm vs. 3–11 ppm).

The Voltage flow is most similar to Tims

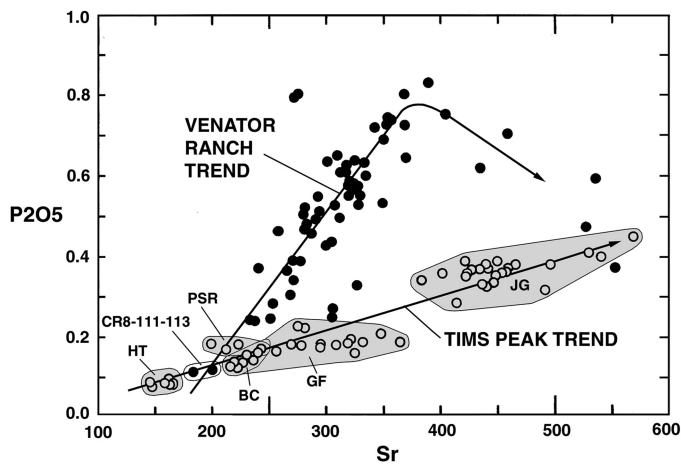
Peak chemistry; they have comparable major and trace element values and similar Mg numbers. The Drinkwater basalt, however, is both more variable and more evolved (Figs. 15C, 15D); it has slightly lower Mg numbers, significantly lower Ni contents, and variable incompatible element values that most likely reflect the modification of more primitive magmas by crystal fractionation and/or crustal contamination.

Hirose and Kushiro (1993) demonstrated that high-Al<sub>2</sub>O<sub>3</sub> basalts can be generated by small degrees of melting of mantle peridotite. In support of the earlier observations of McKee et al. (1983) and Hart and Carlson

(1987), Draper (1991) presented experimental data showing that the HAOT lavas of eastern Oregon probably underwent only moderate fractionation from melts of mantle peridotite at moderate pressure (15–20 kbar). Indeed, the primitive nature of the Tims Peak and Voltage flows suggest that they may be near-primary melts that have undergone only minor modification prior to eruption.

Eruption of the diktytaxitic basalts may delineate periods of enhanced extension, which allowed these mafic melts to rise quickly from the mantle, with little residence time in the crust. Such rapid ascent rates may be an inherent genetic trait of diktytaxitic lavas. Car-

**Figure 16.** Sr vs.  $P_2O_5$  for Venator Ranch basalt and various chemical types of Tims Peak basalt. HT—Hat Top (Hooper et al., 2002a); PSR—Pence Spring Reservoir (Hooper et al., 2002a); BC—Bull Canyon type (this study); GF—Grasshopper Flat (Binger, 1997; and this study); JG—Juniper Gulch (Hooper et al., 2002a).



off et al. (2000), for example, argued that rapid ascent leaves little time for water-saturated magma to degas, so that degassing takes place at the surface, thus generating diktytaxitic textures (Goff, 1996).

#### The Intermediate Rocks (Keeney Sequence)

Intermediate-composition lavas of the Keeney sequence are readily distinguished from all other rock types by their lower  $TiO_2/P_2O_5$  ratios (Fig. 13C) and their higher Sr contents (400–800 ppm). As a group, they comprise basaltic andesites, andesites, basaltic trachyandesites, and trachyandesites (Fig. 17B). Of the three chemical subtypes, the trachyandesite of Cobb Creek is notably distinct in both major and trace element composition (Table 1; Figs. 13 and 14). These lavas display particularly high Zr values (260–280 ppm) with respect to moderately low values of  $SiO_2$  (53%–56.7%) and Mg# (35–40) (Figs. 15C, 15D). Although the basaltic andesite of Buck Mountain and the trachyandesite of Riverside have overlapping ranges for major elements and most trace elements, they can be readily distinguished from one another by their Zr, Sr, and  $TiO_2/P_2O_5$  ratios (Figs. 13C, 15C, 15D).

The Keeney sequence lavas are best described as being calc-alkaline to mildly alkaline, based on variations in FeO and alkalinity (Figs. 17A and 17B). The Cobb Creek lavas, the most alkalic of the three types, have tholeiitic affinities, in that they display high FeO/MgO ratios at moderate  $SiO_2$  contents (Fig. 14B). However, they do not display the characteristic Fe-enrichment trend of tholeiitic magmas, but rather a calc-alkaline trend similar to the Buck Mountain and Riverside lavas.

The generation of calc-alkaline magma is

typically attributed to subduction-zone processes, which begin with lowering of the peridotite solidus by  $H_2O$  and other volatiles escaping from subducting oceanic crust (Gill, 1981; Davis and Stevenson, 1992). The high water content of subduction-related magma suppresses plagioclase as a liquidus phase and promotes the crystallization of hornblende and magnetite (Sisson and Grove, 1993). Removal of these Fe-rich phases leads to a progressive calc-alkaline trend, defined by its lack of Fe enrichment.

This scenario, however, cannot be applied to the Keeney sequence lavas, which were generated in an environment of continental extension, far removed from the steeply dipping Juan de Fuca plate to the west. These calc-alkaline lavas are more alkalic than the basaltic andesites and andesites found in typical subduction-related settings. Processes unrelated to subduction must be invoked to explain their unusual association of moderately high alkalinity, combined with a lack of Fe enrichment, in an extensional tectonic setting.

The Keeney sequence lavas in the map area are typically fine grained and aphyric; they lack any chemical evidence of significant fractional crystallization. Their major and trace element analyses lie along disparate trends unrelated to crystallization trends displayed by the mapped basaltic rock types (Fig. 18). All three subtypes maintain exceptionally narrow ranges in Zr, a HFS incompatible element that should increase in the melt during fractional crystallization. In contrast, the LIL elements (Ba, Rb, Sr, K) display wide compositional ranges, particularly notable in the Buck Mountain and Riverside lavas (Figs. 18A and 18B). The 36 Buck Mountain lavas, for example, display a Zr range from 189 to 209 ppm, but a Ba range from 842 to 1722 ppm.

The decoupling of the HFS and LIL elements cannot be explained by fractional crystallization. However, these variations are compatible with crustal contamination, or magma mixing, with a high-silica granitic source. Such a model is consistent with small crustal xenoliths found in the Riverside lavas (Hanson, 1998), and we infer that it provides a viable mechanism for generating both the moderately high alkalinity of the Keeney sequence lavas and their resultant calc-alkaline trend. The lack of Fe enrichment in these rocks (Fig. 14) may be less the product of hornblende and magnetite crystallization and more the result of mixing between basaltic to andesitic magmas and high-silica, low-Fe, granitic sources. Such mixing processes are ubiquitous in the 10.4 Ma Duck Butte eruptive center, ~15 km southeast of the map area (Johnson and Grunder, 2000). A similar scenario for generating extension-related calc-alkaline lavas was suggested by Hawkesworth et al. (1995) for an analogous suite of rocks in the southern part of the Basin and Range province.

#### The Felsic Rocks

The felsic rock types include the older Oligocene–Miocene dacites, the widespread Dinner Creek and Devine Canyon tuffs, the felsic eruptive centers, and their outflow facies. Most of these rocks are high-silica rhyolites ( $SiO_2 = 73\%–80\%$ ). The only dacitic rocks are the older Oligocene–Miocene dacites, and those from the South Fork eruptive center (Fig. 3). Numerous basaltic andesite inclusions are the distinctive feature of the South Fork dacite. Similar inclusions are found in the nearby Duck Butte eruptive center, which as already noted, formed from a series of felsic eruptions associated with periodic mixing and commingling of more mafic magma (Johnson and Grunder, 2000). The wide range in  $SiO_2$  values (60%–70.7%) for the South Fork dacite may suggest a similar origin; however, this conjecture must await more thorough study.

All of the rhyolites plot near the low-pressure thermal minimum on the normative Ab-Or-Qtz diagram of Tuttle and Bowen (1958), suggesting that they were derived either by considerable crystal fractionation or by crustal anatexis. Mass-balance and geophysical constraints argue against extreme fractionation for the largest of these rhyolite bodies (Draper, 1991), and there is little petrographic or chemical evidence to support such an origin. It is difficult to reconcile a simple model of crystal fractionation with the wide compositional diversity of these rocks, as demonstrated in the

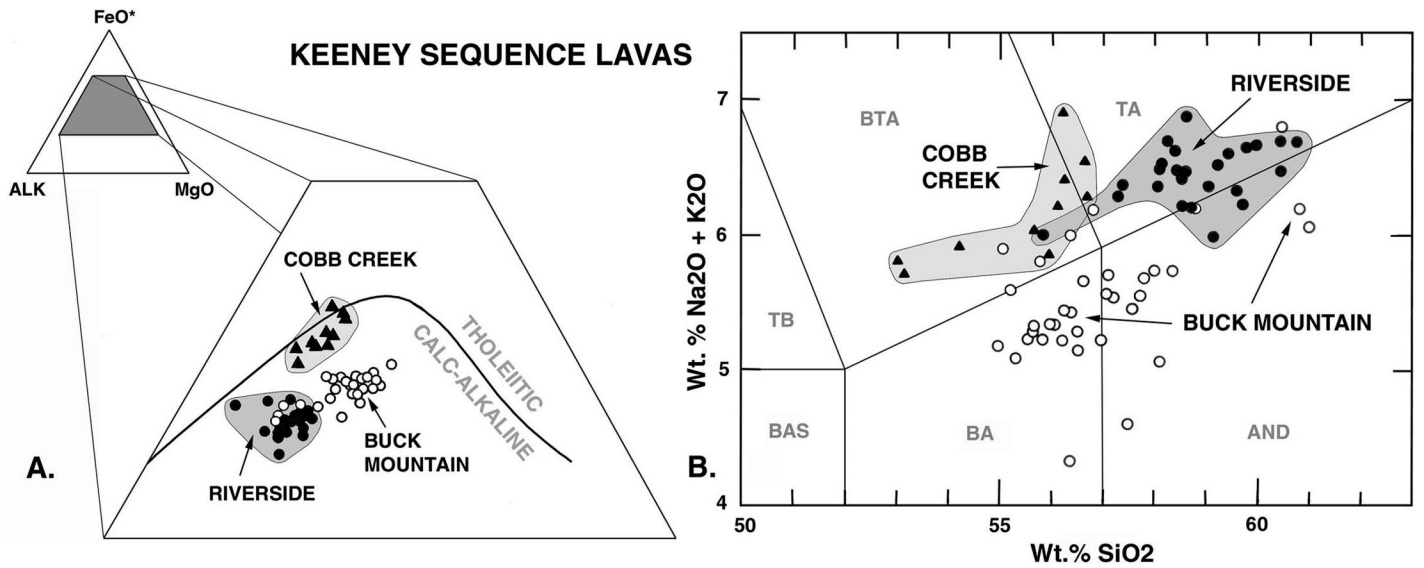


Figure 17. Compositional variations of the Keeney sequence lavas, and their calc-alkaline to mildly alkaline character, are illustrated in (A) the AFM ( $\text{Al}_2\text{O}_3\text{-FeO-MgO}$ ) diagram of Irvine and Baragar (1971), and (B) the total alkali vs. silica plot of LeBas et al. (1986). Compositional abbreviations: BAS—basalt; BA—basaltic andesite; AND—andesite; TB—trachybasalt; BTA—basaltic trachyandesite; TA—trachyandesite.

Ba-Zr diagram (Fig. 19). If these rhyolites are indeed derived from crustal anatexis, then the trace element data suggest that the source rocks themselves may be highly variable in composition. This possibility is consistent with the heterogeneous nature of the crust lying west of the North American craton (Fig. 1), which is likely to be a combination of oceanic- and entrained continental protoliths (Leeman et al., 1992).

The injection of basaltic magma beneath the McDermitt caldera (Fig. 1) initiated crustal melting and the subsequent eruption of per-alkaline rhyolites at ca. 16.6 Ma (Rytuba and McKee, 1984; Swisher et al., 1990). Rhyolitic magmatism appears to have progressed northward into the map area, with sporadic Miocene eruptions that may have begun at the Swamp Creek eruptive center at ca. 15.7 Ma (Fig. 3). These early eruptions north of

McDermitt also include those associated with the ca. 15.5 Ma Mahogany Mountain and Three Fingers calderas ~55 km east of the map area in the Oregon-Idaho graben (Cummings et al., 2000). Still farther north are the younger eruptions of the rhyolitic Hog Creek sequence along the northwestern margin of the Oregon-Idaho graben at ca. 15.3 Ma (Hooper et al., 2002a) and the contemporaneous eruption of the Dinner Creek tuff from near the

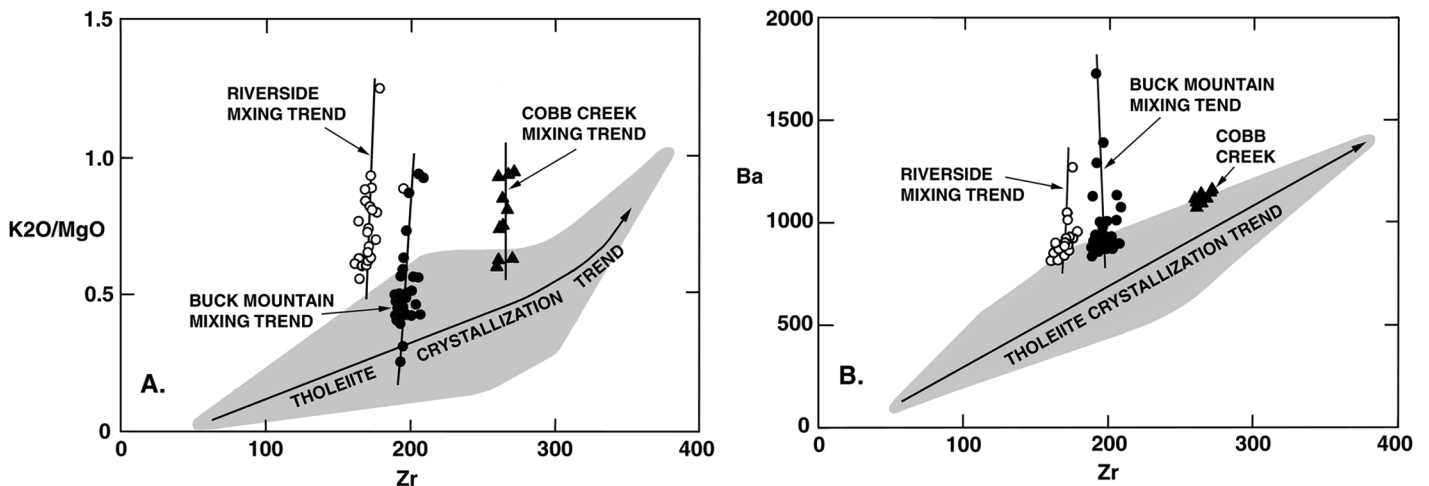
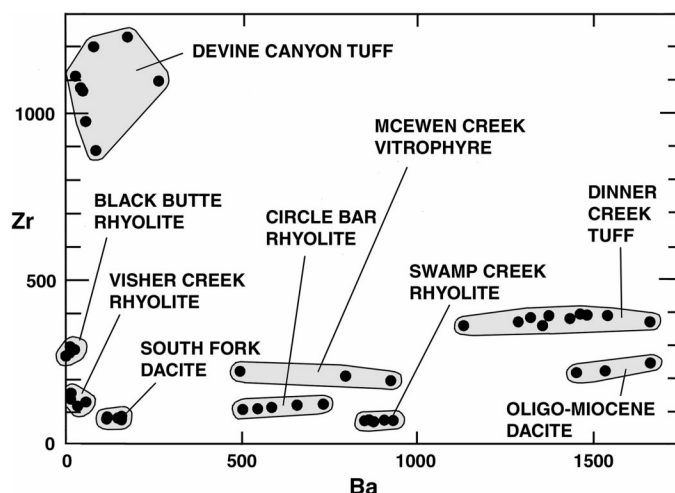


Figure 18. Variation diagrams showing the relative behavior of large-ion lithophile elements vs. Zr, a high field strength element. (A) Zr vs.  $\text{K}_2\text{O/MgO}$ . (B) Zr vs. Ba. The undifferentiated Steens, basalt of Malheur Gorge, Hunter Creek, and Venator Ranch analyses (shaded area) vary along broad trends that typify basaltic crystallization in both diagrams. The Keeney sequence lavas (Cobb Creek, Riverside, and Buck Mountain), however, show wide variations in the LILE with very little variation in Zr. Such trends are atypical of fractional crystallization and indicate that a mixing process was involved in the genesis of the Keeney sequence lavas.

Figure 19. The felsic rock types span a wide range of compositions, particularly evident in their trace element ratios, exemplified here by variations in Ba and Zr.



Castle Creek caldera, ~35 km north of the map area (Rytuba and Vander Meulen, 1991; Evans and Binger, 1997). The implied rapid northward advance of basalt injection adjacent to the North American craton is in agreement with stratigraphic data that flood-basalt volcanism progressed northward with time (Camp, 1995; Hooper et al., 2002a). The identification of a systematic progression of rhyolite magmatism, however, is complicated by a superimposed younger period of rhyolitic volcanism that began near the Duck Butte eruptive center at ca. 10.4 Ma (Johnson and Grunder, 2000) and progressed westward along the Brothers fault zone (Streck et al., 1999).

#### IMPLICATIONS OF THE STEENS BASALT–COLUMBIA RIVER BASALT GROUP CONNECTION

The 16.6–15.3 Ma period of tholeiitic volcanism in eastern Oregon was quickly followed by, and overlapped with, the eruption of ~85% of the Columbia River Basalt Group (the Imnaha and Grande Ronde Basalt Formations) (Tolan et al., 1989) between 16.1 and 15.0 Ma (Swisher et al., 1990; Hooper et al., 2002a). Within this tholeiitic province, Binger (1997) and Hooper et al. (2002a) have demonstrated that the lower Pole Creek basalt (basalt of Malheur Gorge) is chemically indistinguishable from the lower Steens basalt to the south, the upper Pole Creek basalt (basalt of Malheur Gorge) is chemically indistinguishable from Imnaha Basalt (Columbia River Basalt Group) to the north, and the overlying Birch Creek and Hunter Creek basalts are chemically indistinguishable from Grande Ronde Basalt (Columbia River Basalt Group). The data presented here demonstrate that (1)

the upper Steens basalt thins to the north from Steens Mountain through the map area before pinching out entirely near Juntura, (2) the lower Steens basalt flows continue northward from Steens Mountain and are physically connected to the lower Pole Creek lavas immediately south of the Juntura Quadrangle (Fig. 7), and (3) lavas of upper Pole Creek and Birch Creek chemistry (generally those analyses with  $\text{SiO}_2 > 51.5\%$ , Fig. 12C) are present throughout the map area but pinch out to the south, along the northern margin of Steens Mountain.

The physical and chemical linkage of these Columbia River Basalt–equivalent lavas into eastern Oregon has some significant implications. Models of flood-basalt volcanism in the Pacific Northwest can no longer consider the Columbia Plateau basalts in isolation. Such models require revisions in both volume estimates and magma-supply rates for Columbia River Basalt volcanism. A conservative estimate of the Steens basalt–basalt of Malheur Gorge volume is 60,000 km<sup>3</sup> (Carlson and Hart, 1988). This expands the known volume of Columbia River flood-basalt volcanism by >25%, from ~174,000 km<sup>3</sup> (Tolan et al., 1989) to 234,000 km<sup>3</sup>. Grande Ronde Basalt was thought to comprise ~85% of the total volume, and Imnaha basalt, ~5% (Tolan et al., 1989). The addition of the Imnaha-equivalent upper Pole Creek basalt to the Columbia River Basalt Group volume, together with the stratigraphically linked lower Pole Creek and Steens basalt, decreases the Grande Ronde basalt volume to ~63.5% of the total and increases the Imnaha-equivalent and older lavas to ~30% of the total.

The added volume of these early flows suggests that the magma supply rates for Columbia River Basalt Group volcanism, and partic-

ularly its early phase, are higher than previously estimated. The new <sup>40</sup>Ar/<sup>39</sup>Ar dates of Hooper et al. (2002a) indicate that the greatest volume of flood-basalt volcanism (220,500 km<sup>3</sup>) occurred over an interval of 1.3 m.y. This equates to a magma supply rate of 0.17 km<sup>3</sup>/yr, which is comparable to the current magma supply rate of 0.18 km<sup>3</sup>/yr above the Hawaiian hotspot (Pyle, 2000).

#### SUMMARY OF EVENTS

The map relationships described herein provide the means for establishing stratigraphic correlations across a broad area of eastern Oregon. The generalized cross section of Figure 20 depicts these lateral correlations, from Steens Mountain in the south (Johnson et al., 1998a), through the map area, into the Malheur River Gorge (Hooper et al., 2002a), and farther north to the source region of the Columbia River Basalts.

The Oligocene–Miocene volcanic rocks exposed in the map area, and at scattered locations throughout eastern Oregon, record a poorly known period of calc-alkaline volcanism. Several workers have argued that calc-alkaline volcanism in the inland Pacific Northwest is not related to subduction, but rather to decompressional partial melting associated with continental extension (Robyn, 1979; Bailey, 1990; Hooper et al., 1995). Whatever the mechanism, it is apparent that the calc-alkaline eruptions at Steens Mountain were separated from the subsequent flood-basalt eruptions by only a short time interval (<1.5 m.y.).

The paleomagnetic data from Mankinen et al. (1987) indicate that the initial reverse-polarity eruptions of Steens basalt were dispersed over a broad region of southeastern Oregon and that later eruptions became more localized, culminating in a shield-building stage of normal-polarity lavas concentrated at Steens Mountain (Johnson et al., 1998a). These observations are consistent with the field and petrochemical correlations presented here. The initial, flood-basalt eruptions began at ca. 16.6 Ma, extending from near Steens Mountain, through the map area, and farther north (Fig. 20; lower Steens and lower Pole Creek basalts). At Steens Mountain these eruptions became increasingly more alkalic with time (upper Steens basalt). The upper Steens basalt flows decrease northward and are not present beyond the map area (Fig. 20). Eruption of the upper Steens basalt to the south, and upper Pole Creek basalt to the north, appears to be at least partly contemporaneous, with both types interbedded with one another throughout the map area.

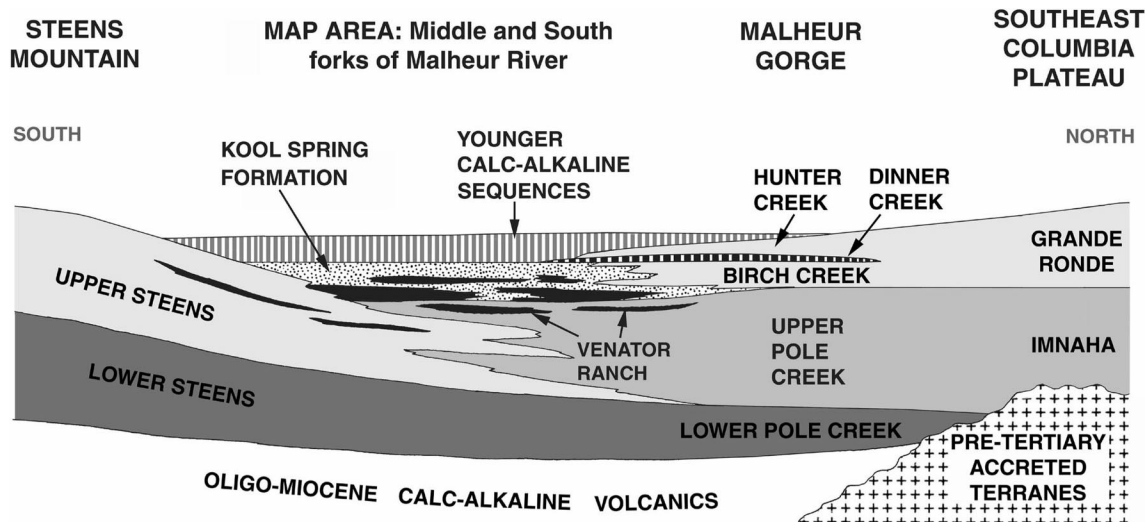


**Figure 20.** Generalized schematic cross section from Steens Mountain in the south, through the map area, to the Columbia Plateau in the north. Regional stratigraphic relationships are based on the mapping and petrochemical data presented here and on a variety of mapping and petrochemical studies summarized in Hooper et al. (2002a).

Petrochemical variations suggest that the upper Pole Creek lavas were derived from the same mantle source as the more primitive lower Pole Creek lavas (lower Steens basalt) and that fractional crystallization of these magma types has played a dominant role in generating the overlying Birch Creek and Hunter Creek basaltic andesites. Whereas lavas of Birch Creek chemistry are scattered throughout the map area, generally at the top of collected sections, Hunter Creek basalt appears to be restricted to the northern part. The field distribution of the entire tholeiitic sequence north of Steens Mountain is consistent with an overall northward migration of flood-basalt volcanism with advancing time.

The 16.6–15.3 Ma period of Steens-type eruptions was punctuated in the map area by partly contemporaneous eruptions of Venator Ranch basalt and felsic pyroclastic units entrained in the Kool Spring formation and Dinner Creek tuff (Fig. 20). Interbedded in the upper half of the flood-basalt sequence, the Venator Ranch basalt flows increase in abundance from the Steens Mountain section, to the Summit Springs section, and into the map area, where they are overlain by, and incorporated within, the Kool Spring formation (Figs. 6 and 20). Primarily derived from local sources, this bimodal succession appears to be restricted to a poorly defined structural depression lying north of the presumed shield-volcano edifice of Steens Mountain.

In the southern part of the map area, the Kool Spring formation is overlain by a thin, isolated outcrop of the 15.3 Ma Dinner Creek tuff. Both the Dinner Creek tuff and the over-

lying Hunter Creek basalt thicken to the north where they are largely confined to outcrops in the Juntura Quadrangle (Fig. 7). Like the Venator Ranch–Kool Spring association, the Dinner Creek–Hunter Creek relationship reflects a period of bimodal eruption, associated in time with additional rhyolitic eruptions along the margin the Oregon-Idaho graben (Cummings et al., 2000). The field evidence indicates that the waning stages of the flood-basalt volcanism in the map area, and farther east, were associated with an enhanced period of continental extension affiliated with graben formation and bimodal eruptions.

The period of graben initiation at ca. 15.5–15.3 Ma marks a transition from voluminous eruptions of tholeiitic flood basalt, to sporadic, small-volume eruptions of calc-alkaline lava. The initial eruptions were of primitive lava, manifested in the various chemical subtypes of Tims Peak basalt. These mafic eruptions, grossly centered ca. 13.5 Ma, were followed by the eruption of intermediate-composition, calc-alkaline lava of the Keeney sequence from ca. 13 to 10 Ma and by eruption of the Devine Canyon tuff at ca. 9.7 Ma.

Field relationships demonstrate that extension continued in the map area during and following the eruptions Tims Peak basalt and the Keeney sequence lavas. Extension was manifested in development of numerous normal faults, largely along northwest and north trends, and by the creation of structurally controlled basins of deposition (e.g., the Juntura Basin, Fig. 3). Similarly, the onset of calc-alkaline volcanism in the Oregon-Idaho graben was marked by the development of intra-

graben fault zones associated with the creation of distinct subbasins (Cummings et al., 2000). Although prolonged periods of continental extension are normally associated with regional subsidence, the development of canyons deeper than 500 m indicates that vigorous uplift was taking place, at least on a local scale. These drainages were subsequently filled by the Buck Mountain and Riverside intracanyon lava flows.

The final eruptive products in the map area were the Drinkwater flows at ca. 7.0 Ma and the Voltage flow before 32,000 yr B.P. These lavas are compositionally distinct from those of the Keeney sequence, but similar in composition to the more primitive, diktytaxitic Tims Peak basalt. In contrast to the 9.7 Ma Devine Canyon tuff, which is offset and tilted substantially by numerous normal faults, the Drinkwater lavas form gently tilted mesas cut by only a few normal faults with very little displacement. The evidence suggests that crustal extension since ca. 7.0 Ma has been much less severe than in previous episodes.

#### REGIONAL TECTONO-MAGMATIC CONSIDERATIONS

Discourse on the genesis of flood-basalt volcanism in the Pacific Northwest has involved both plume and nonplume interpretations. King and Anderson (1995) have suggested that continental flood basalts could be derived from upper-mantle convection along the boundary between two lithospheric plates of contrasting thickness. Under this scenario, the potential for generating a high volume of

magma could be enhanced by decompression-  
al melting associated with either backarc extension (Carlson and Hart, 1987) or torsional stress of the plate interior (Dickinson, 1997). Teleseismic studies of the upper mantle beneath the Snake River Plain (Fig. 1) are compatible with both plume and nonplume origins (Humphreys et al., 2000). It is our contention, however, that the sudden outburst of Steens basalt eruptions, over an exceedingly short time span of ~1.3 m.y., requires the abrupt arrival of a hot mantle source. A growing body of evidence supports the idea that this flood-basalt event was directly related to emplacement of the Yellowstone mantle plume beneath the McDermitt caldera complex at ca. 16.6 Ma (Fig. 1) (Brandon and Goles, 1988; Draper, 1991; Pierce and Morgan, 1992; Hooper and Hawkesworth, 1993; Dodson et al., 1997; Takahashi et al., 1998; Hooper et al., 2002a).

Most workers have embraced the idea that flood-basalt provinces are generated above starting plume heads and that hotspot tracks are generated above the feeding plume tails (Morgan, 1981; Courtillot et al., 1986; Olson and Nam, 1986; Richards et al., 1989; Campbell and Griffiths, 1990; Griffiths and Campbell, 1991; Olson, 1990; Hill et al., 1992; Weinberg, 1997). If these models are correct, then it is more than coincidental that the McDermitt caldera neatly separates flood-basalt volcanism to the north (underlain by the supposed plume head), from the Yellowstone hotspot track to the east (underlain by the supposed plume tail) (Fig. 1). This unique geographic association has led several workers to conclude that the plume head was sheared off against the westward-moving Precambrian craton shortly after its emplacement (Draper, 1991; Pierce and Morgan, 1992; Parsons et al., 1994), thereby allowing the plume tail to generate a hotspot track through the overriding craton.

Geophysical data demonstrate that continental plume heads pond at the base of the lithosphere, where they spread preferentially into areas of thin lithosphere, often along distinct pathways of concentrated mantle flow (Thompson and Gibson, 1991; Sleep, 1997). It therefore seems reasonable to conclude that the thick cratonic margin of North America would have acted as a buttress that blocked the spreading Yellowstone plume head, thus channelizing flow into a parallel passage beneath the adjacent, thinner oceanic lithosphere (Camp, 1995).

The chemical correlations and stratigraphic data presented here and elsewhere (Lees, 1994; Binger, 1997; Johnson et al., 1998a;

Cummings et al., 2000; Hooper et al., 2002a) allow us to test the efficacy of such models as they apply to flood-basalt volcanism in eastern Oregon. Most models of plume impingement predict that a period of thermal uplift should precede plume-induced extension and flood-basalt volcanism (Campbell and Griffiths, 1990; Hill et al., 1992). Well-developed angular unconformities in the map area and at the base of Steens Mountain (Langer, 1991) demonstrate that such uplift may have occurred during the brief hiatus (ca. 1.5 Ma) separating the last Oligocene–Miocene eruptions from the first eruptions of Steens basalt. North of the map area, Goles (1986) has presented similar evidence for the onset of regional-scale uplift after the last eruptions of the John Day Formation (early Miocene) and before the first eruptions of the Columbia River Basalt Group.

The focus of uplift, both during and preceding flood-basalt eruption, appears to have been centered near McDermitt, along the Oregon-Nevada border (Parsons et al., 1994), where the entire 900-m-thick lava section exposed at Steens Mountain pinches out over a short lateral distance of <100 km. The earliest lavas of lower Steens basalt spread rapidly to the north and northwest, filling the newly formed paleotopography across much of southeastern Oregon. Subsequent eruptions north of Steens Mountain, however, resulted in the progressive offlap of upper Pole Creek basalt, Birch Creek basalt, and Hunter Creek basalt, all of which thicken northward from the map area toward the Chief Joseph dike swarm (Fig. 20), where they are known as the Imnaha and Grande Ronde Basalt Formations. This offlapping relationship of progressively younger flood-basalt successions to the north (Fig. 20) could be attributed to (1) progressive uplift generating a northward-tilting paleoslope, (2) a northward migration of flood-basalt eruption, or (3) a combination of both.

A remarkably similar migratory pattern is evident in these same units, and in progressively younger Columbia River Basalt Group units, from the southeastern Columbia Plateau. Here, similar northward-offlapping relationships of Imnaha Basalt and each of the four magnetostratigraphic units of Grande Ronde Basalt have been attributed to the regression of lavas against a regional paleoslope that continued to emerge throughout the period of Columbia River Basalt eruption (Camp, 1995). This progressive uplift was accompanied by the overall migration of flood-basalt eruptions from the Chief Joseph dike swarm (Fig. 1), which is demonstrated by a preponderance of Imnaha Basalt dikes in the

south, progressively more Grande Ronde Basalt dikes to the north, and the restriction of the youngest dikes of Wanapum and Saddle Mountains Basalts to the far north of the dike swarm.

This overall pattern of regional uplift, basalt regression, and vent migration across the breadth of eastern Oregon and into southeastern Washington is markedly consistent. Building on previous ideas (Camp, 1995), we interpret this pattern as the surface expression of a spreading mantle-plume head that was sheared and distorted against the cratonic margin, forcing its rapid propagation to the north. Plume propagation to the south was inhibited by a broad transition zone of continental lithosphere in northern Nevada (Pierce and Morgan, 1992), thus generating a smaller volume of contemporaneous volcanic rocks along the Northern Nevada rift zone (Fig. 1).

Initial impingement of the mantle-plume head was associated with uplift that began before the earliest eruptions of Steens basalt. As the plume head spread outward, its flow became channelized beneath the thin oceanic lithosphere, adjacent to the thick continental lithosphere of the Precambrian craton. The progressive deflection of this hot mantle beneath northeastern Oregon and into adjacent Washington was accompanied by the rapid northward migration of thermally driven uplift, which was both coincident and contemporaneous with a similar migration of flood-basalt eruption.

#### ACKNOWLEDGMENTS

We are grateful for the conscientious reviews provided by Bill Hart and Peter Hooper. We are especially indebted to Diane Johnson of the Geo-Analytical Lab at Washington State University for performing the XRF analyses, and for providing us with patient, professional guidance in the preparation of the XRF and ICP-MS analyses. We thank Jenda Johnson for introducing Camp and Hanson to the geology of southeastern Oregon and for assisting in the collection of reconnaissance samples. We thank Jenda and Jim Evans for sharing their field data and supplying us with maps of adjacent quadrangles. The  $^{40}\text{Ar}/^{39}\text{Ar}$  radiometric date for the trachyandesite of Riverside was kindly provided by Doug Pyle. Northeastern University provided financial support for Marty Ross, and helped to defray the cost of chemical analyses and thin sections.

#### REFERENCES CITED

- Armstrong, R.L., Taubeneck, W.P., and Hales, P.O., 1977, Rb-Sr and K-Ar geochronometry of Mesozoic granitic rocks and their Sr isotopic composition, Oregon, Washington, and Idaho: *Geological Society of America Bulletin*, v. 88, p. 397–411.
- Bailey, D.G., 1990, Geochemistry and petrogenesis of Miocene volcanic rocks in the Powder River volcanic field, northeastern Oregon [Ph.D. thesis]: Pullman, Washington State University, 341 p.

- Baksi, A.K., Hall, C.H., and York, D., 1991, Laser probe  $^{40}\text{Ar}/^{39}\text{Ar}$  dating studies on submilligram whole-rock basalt samples: The age of the Steens Mountain geomagnetic polarity transition (revisited): *Earth and Planetary Science Letters*, v. 104, p. 292–298.
- Binger, G.B., 1997, The volcanic stratigraphy of the Juntura region, eastern Oregon [M.S. thesis]: Pullman, Washington State University, 206 p.
- Brandon, A.D., and Goles, G.G., 1988, A Miocene subcontinental plume in the Pacific Northwest: Geochemical evidence: *Earth and Planetary Science Letters*, v. 88, p. 273–283.
- Brooks, H.C., Ferns, M.L., Nusbaum, R.W., and Kovich, P.M., 1979, Geologic map of the Rastus Mountain Quadrangle, Oregon: Oregon Department of Geology and Mineral Industries Open-File Report O-79-07, scale 1:24,000.
- Brueseke, M.E., and Hart, W.K., 2000, Reevaluation and new age constraints on the eruptive history of the mid-Miocene Steens basalt, southeastern Oregon: *Geological Society of America Abstracts with Programs*, v. 32, no. 7, p. A-142.
- Camp, V.E., 1981, Geologic studies of the Columbia Plateau: Part II. Upper Miocene basalt distribution, reflecting source locations, tectonism, and drainage history in the Clearwater embayment, Idaho: *Geological Society of America Bulletin*, v. 92, p. 669–678.
- Camp, V.E., 1995, Mid-Miocene propagation of the Yellowstone mantle plume head beneath the Columbia River basalt source region: *Geology*, v. 23, p. 435–438.
- Camp, V.E., and Hooper, P.R., 1981, Geologic studies of the Columbia Plateau: Part I. Late Cenozoic evolution of the southeastern part of the Columbia River basalt province: *Geological Society of America Bulletin*, v. 92, p. 659–668.
- Camp, V.E., and Roobol, M.J., 1992, Upwelling asthenosphere beneath western Arabia and its regional implications: *Journal of Geophysical Research*, v. 97, p. 15,255–15,271.
- Camp, V.E., and Ross, M.E., 2000, Mapping the Steens–Columbia River Basalt (CRB) connection: Implications for the extent, volume, and magma supply rate of CRB volcanism: *Geological Society of America Abstracts with Programs*, v. 32, no. 7, p. A-159.
- Campbell, I.H., and Griffiths, 1990, Implications of mantle plume structure for the evolution of flood basalts: *Earth and Planetary Science Letters*, v. 99, p. 79–93.
- Carlson, R.W., and Hart, W.K., 1987, Crustal genesis on the Oregon Plateau: *Journal of Geophysical Research*, v. 92, p. 6191–6206.
- Carlson, R.W., and Hart, W.K., 1988, Flood basalt volcanism in the Pacific northwestern United States, in Macdougall, J.D., ed., *Continental flood basalts: Dordrecht, Netherlands, Kluwer Academic Publishers*, p. 35–62.
- Caroff, M., Maury, R.C., Cotten, J., and Clement, J.-P., 2000, Segregation structures in vapor-differentiated basaltic flows: *Bulletin of Volcanology*, v. 62, p. 171–187.
- Clague, D.A., 1987, Hawaiian alkaline volcanism: Fitton, J.G., and Upton, B.G.J., eds., *Alkaline igneous rocks: Oxford, Blackwell*, p. 227–252.
- Courtilot, V., Besse, J., Vandamme, E., Montigny, R., Jaeger, J.-J., and Cappeta, H., 1986, Deccan flood basalts at the Cretaceous-Tertiary boundary: *Earth and Planetary Science Letters*, v. 80, p. 361–374.
- Cummings, M.L., Evans, J.G., Ferns, M.L., and Lees, K.R., 2000, Stratigraphic and structural evolution of the middle Miocene synvolcanic Oregon-Idaho graben: *Geological Society of America Bulletin*, v. 112, p. 668–682.
- Davis, J.H., and Stevenson, D.J., 1992, Physical model of source region of subduction zone volcanics: *Journal of Geophysical Research*, v. 97, p. 2037–2070.
- Dickinson, W.R., 1997, Overview: Tectonic implications of Cenozoic volcanism in coastal California: *Geological Society of America Bulletin*, v. 109, p. 936–954.
- Dodson, A., Kennedy, B.M., and DePaolo, D.J., 1997, Helium and neon isotopes in the Innaha basalt, Columbia River Basalt Group: Evidence for a Yellowstone plume source: *Earth and Planetary Science Letters*, v. 150, p. 443–451.
- Draper, D.S., 1991, Late Cenozoic bimodal magmatism in the northern Basin and Range province of southeastern Oregon: *Journal of Volcanology and Geothermal Research*, v. 47, p. 299–328.
- Eaton, G.P., 1984, The Miocene Great Basin of western North America as an extended back-arc region: *Tectonophysics*, v. 102, p. 275–295.
- Ekren, E.B., McIntyre, D.H., Bennett, E.H., and Malde, H.E., 1981, Geologic map of Owyhee County, Idaho, west of longitude 116°W: U.S. Geological Survey Miscellaneous Investigations Map I-1256, scale 1:250,000.
- Evans, J.G., 1990, Geology and mineral resources map of the South Mountain Quadrangle, Malheur County, Oregon: Oregon Department of Geology and Mineral Industries Geological Map Series GMS-67, scale 1:24,000.
- Evans, J.G., and Binger, G.B., 1997, Geologic map of the Westfall Butte Quadrangle, Malheur County, Oregon: U.S. Geological Survey Open-File Report 97-481, scale 1:24,000.
- Evans, J.G., and Binger, G.B., 1998, Geologic map of the Little Black Canyon Quadrangle, Malheur County, Oregon: U.S. Geological Survey Open-File Report 98-493, scale 1:24,000.
- Ferns, M.L., Brooks, H.C., Evans, J.G., and Cummings, M.L., 1993a, Geologic map of the Vale 30 × 60 minute quadrangle, Malheur County, Oregon, and Owyhee County, Idaho: Oregon Department of Geology and Mineral Industries Geological Map Series GMS-77, scale 1:100,000.
- Ferns, M.L., Evans, J.G., and Cummings, M.L., 1993b, Geologic map of the Mahogany Mountain 30 × 60 minute quadrangle, Malheur County, Oregon, and Owyhee County, Idaho: Oregon Department of Geology and Mineral Industries Geological Map Series GMS-77, scale 1:100,000.
- Fiebelkorn, R.B., Walker, G.W., MacLeod, N.S., McKee, W.H., and Smith, J.G., 1983, Index to K-Ar determinations for the state of Oregon: *Isochron/West*, v. 37, p. 3–60.
- Gehr, K.D., and Newman, T.M., 1978, Preliminary note on the late Pleistocene geomorphology and archaeology of the Harney Basin, Oregon: *The Ore Bin*, v. v0, no. 10, p. 165–170.
- Gill, J.B., 1981, *Orogenic andesites and plate tectonics*: New York, Springer-Verlag, 358 p.
- Goff, F., 1996, Vesicle cylinders in vapor-differentiated basalt flows: *Journal of Volcanology and Geothermal Research*, v. 71, p. 167–185.
- Goles, G.G., 1986, Miocene basalts of the Blue Mountains province in Oregon: I. Compositional types and their geological settings: *Journal of Petrology*, v. 27, part 2, p. 495–520.
- Green, D.H., and Ringwood, A.E., 1967, The stability fields of aluminous pyroxene peridotite and garnet peridotite and their relevance in the upper mantle: *Earth and Planetary Science Letters*, v. 2, p. 151–160.
- Greene, R.C., Walker, G.W., and Corcoran, R.E., 1972, Geologic map of the Burns quadrangle, Oregon: U.S. Geological Survey Miscellaneous Investigations Map I-680, scale 1:250,000.
- Griffiths, R.W., and Campbell, I.H., 1991, On the dynamics of long-lived plume conduits in the convecting mantle: *Earth and Planetary Science Letters*, v. 103, p. 214–227.
- Gunn, B.M., and Watkins, N.D., 1970, Geochemistry of Steens Mountain basalts, Oregon: *Geological Society of America Bulletin*, v. 81, p. 1497–1516.
- Hanson, W.E., 1998, Volcanic stratigraphy and geologic evolution of Riverside, Oregon, [M.S., thesis]: San Diego, California, San Diego State University, 90 p.
- Hart, W.K., and Carlson, R.W., 1985, Distribution and geochronology of Steens Mountain type basalts from the northwestern Great Basin: *Isochron/West*, no. 43, p. 5–10.
- Hart, W.K., and Carlson, R.W., 1987, Tectonic controls on magma genesis and evolution in the northwestern United States: *Journal of Volcanology and Geothermal Research*, v. 32, p. 119–135.
- Hart, W.K., Aronson, J.L., and Mertzman, S.A., 1984, Areal distribution and age of low-K, high alumina olivine tholeiitic magmatism in the northwestern Great Basin: *Geological Society of America Bulletin*, v. 95, p. 185–195.
- Hart, W.K., Carlson, R.W., and Mosher, S.A., 1989, Petrogenesis of the Pueblo Mountains basalt, southeastern Oregon and northern Nevada, in Reidel, S.P., and Hooper, P.R., eds., *Volcanism and tectonism in the Columbia River flood-basalt province*: *Geological Society of America Special Paper 239*, p. 367–378.
- Hawkesworth, C., Turner, S., Gallagher, K., Hunter, A., Bradshaw, T., and Rogers, N., 1995, Calc-alkaline magmatism, lithospheric thinning and extension in the Basin and Range: *Journal of Geophysical Research*, v. 100, p. 10,271–10,286.
- Hill, R.L., Campbell, I.H., Davies, G.F., and Griffiths, R.W., 1992, Mantle plumes and continental tectonics: *Science*, v. 256, p. 186–193.
- Hirose, K., and Kushiro, I., 1993, Partial melting of dry peridotites at high pressures: Determination of compositions of melts segregated from peridotite using aggregates of diamond: *Earth and Planetary Science Letters*, v. 114, p. 477–489.
- Hooper, P.R., 1997, The Columbia River flood basalt province: Current status, in Mahoney, ed., *Large igneous provinces: Continental, oceanic, and planetary flood basalt volcanism*: *American Geophysical Union Geophysical Monograph 100*, p. 1–27.
- Hooper, P.R., and Camp, V.E., 1981, Deformation of the southeast part of the Columbia Plateau: *Geology*, v. 9, p. 323–328.
- Hooper, P.R., and Hawkesworth, C.J., 1993, Isotopic and geochemical constraints on the origin and evolution of the Columbia River basalt: *Journal of Petrology*, v. 34, p. 1203–1246.
- Hooper, P.R., Bailey, D.G., and McCarley Holder, G.A., 1995, Tertiary calc-alkaline magmatism associated with lithospheric extension in the Pacific Northwest: *Journal of Geophysical Research*, v. 100, p. 10,303–10,319.
- Hooper, P.R., Binger, G.B., and Lees, K.R., 2002a, Constraints on the relative and absolute ages of the Steens and Columbia River basalts and their relationship to extension-related calc-alkaline volcanism in eastern Oregon: *Geological Society of America Bulletin*, v. 114, p. 43–50.
- Hooper, P.R., Johnson, J.A., and Hawkesworth, C.J., 2002b, A model for the origin of the western Snake River Plain as an extensional strike-slip duplex, Oregon-Idaho, in Bonnichsen, B., White, C.M., and McCurry, M., eds., *Tectonic and magmatic evolution of the Snake River Plain volcanic province*: *Idaho Geological Survey Bulletin 30* (in press).
- Humphreys, E.D., Dueker, K.G., Schutt, D.L., and Smith, R.B., 2000, Beneath Yellowstone: Evaluating plume and nonplume models using teleseismic images of the upper mantle: *GSA Today*, v. 10, no. 12, p. 1–6.
- Irvine, T.N., and Baragar, W.R.A., 1971, A guide to the chemical classification of the common volcanic rocks: *Canadian Journal of Earth Sciences*, v. 8, p. 523–548.
- Johnson, J.A., 1995, Geologic evolution of the Duck Creek Butte eruptive center, High Lava Plains, southeastern Oregon [M.S. thesis]: Corvallis, Oregon State University, 151 p.
- Johnson, J.A., and Grunder, A.L., 2000, The making of intermediate composition magma in a bimodal suite: Duck Butte eruptive center, Oregon, USA: *Journal of Volcanology and Geothermal Research*, v. 95, p. 175–195.
- Johnson, J.A., Hawkesworth, C.J., Hooper, P.R., and Binger, G.B., 1998a, Major and trace element analyses of Steens Basalt, southeastern Oregon: U.S. Geological Survey Open-File Report 98-482, 26 p.
- Johnson, J.A., Hooper, P.R., Hawkesworth, C.J., and Binger, G.B., 1998b, Geologic map of the Stenler Ridge quadrangle, Malheur County, southeastern Oregon: U.S. Geological Survey Open-File Report OF 98-105, scale 1:24,000.
- King, S.D., and Anderson, D.L., 1995, An alternative mechanism of flood basalt formation: *Earth and Planetary Science Letters*, v. 136, p. 269–279.
- Kistler, R.W., and Peterman, Z.E., 1978, Reconstruction of

- crustal blocks in California on the basis of initial strontium isotopic compositions of Mesozoic granitic rocks: U.S. Geological Survey Professional Paper 1071, 17 p.
- Kittleman, L.R., Green, A.R., Haddock, G.H., Hagood, A.R., Johnson, A.M., McMurray, J.M., Russell, R.G., and Weeden, D.A., 1965, Cenozoic stratigraphy of the Owyhee region, south-eastern Oregon: University of Oregon Museum of Natural History Bulletin 1, 45 p.
- Langer, V., 1991, Geology and petrologic evolution of the silicic to intermediate volcanic rocks underneath Steens Mountain basalt, southeastern Oregon [M.S. thesis]: Corvallis, Oregon State University, 109 p.
- Laursen, J.M., and Hammond, P.E., 1974, Summary of radiometric ages of Oregon and Washington rocks, through 1972: *Isochron/West*, v. 9, 32 p.
- Lawrence, R.D., 1976, Strike-slip faulting terminates the Basin and Range province in Oregon: *Geological Society of America Bulletin*, v. 87, p. 846–850.
- LeBas, M.J., Le Maitre, R.W., Streckeisen, A., and Zanettin, B., 1986, A chemical classification of volcanic rocks based on total alkali-silica diagram: *Journal of Petrology*, v. 27, pt. 3, p. 745–750.
- Leeman, W.P., Oldow, J.S., and Hart, W.K., 1992, Lithospheric-scale thrusting in the western U.S., Cordillera as constrained by Sr and Nd isotopic transitions in Neogene volcanic rocks: *Geology*, v. 20, p. 63–66.
- Lees, K.R., 1994, Magmatic and tectonic changes through time in the Neogene volcanic rocks of the Vale area, Oregon, northwestern USA [Ph.D. thesis]: Milton Keynes, England, Open University, 284 p.
- Mankinen, E.A., Larson, E.E., Gromme, C.S., Prevot, M., and Coe, R.S., 1987, The Steens Mountain (Oregon) geomagnetic polarity transition: 3. Its regional significance: *Journal of Geophysical Research*, v. 92, p. 8057–8076.
- McKee, E.H., Duffield, W.A., and Stern, R.J., 1983, Late Miocene and early Pliocene basaltic rocks and their implications for crustal structure, northeastern California and south-central Oregon: *Geological Society of America Bulletin*, v. 94, p. 292–304.
- Miyashiro, A., 1974, Volcanic rock series in island arcs and active continental margins: *American Journal of Science*, v. 274, p. 321–355.
- Morgan, W.J., 1981, Hotspot tracks and the opening of the Atlantic and Indian Oceans, in Emiliani, C., ed., *The oceanic lithosphere*: New York, John Wiley, p. 443–487.
- Murphy, J.B., Oppliger, G.L., Bimhall, G.H., and Hynes, A., 1998, Plume-modified orogeny: Example from the western United States: *Geology*, v. 26, p. 731–734.
- Olson, P., 1990, Hot spots, swells and mantle plumes, in Ryan, M.P., ed., *Magma transport and storage*: New York, John Wiley, p. 33–51.
- Olson, P., and Nam, I.S., 1986, Formation of seafloor swells by mantle plumes: *Journal of Geophysical Research*, v. 91, p. 7181–7191.
- Parsons, T., Thompson, G.S., and Sleep, N.H., 1994, Mantle plume influence on the Neogene uplift and extension of the U.S. western Cordillera: *Geology*, v. 22, p. 83–86.
- Pierce, K.L., and Morgan, L.A., 1992, The track of the Yellowstone hot spot: Volcanism, faulting, and uplift, in Link, P.K., et al., eds., *Regional geology of eastern Idaho and western Wyoming*: Geological Society of America Memoir 179, p. 1–53.
- Pyle, D.M., 2000, Sizes of volcanic eruptions: Sigurdsson, H., ed., *Encyclopedia of volcanoes*: San Diego, Academic Press, p. 263–279.
- Reidel, S.P., Tolan, T.L., Hooper, P.R., Beeson, M.H., Fecht, K.R., Bentley, R.D., and Anderson, J.L., 1989, The Grande Ronde Basalt, Columbia River Basalt Group, in Reidel, S.P., and Hooper, P.R., eds., *Stratigraphic descriptions and correlations in Washington, Oregon, and Idaho*: Geological Society of America Special Paper 239, p. 21–54.
- Richards, M.A., Duncan, R.A., and Courtillot, V.E., 1989, Flood basalts and hot-spot tracks: Plume heads and tails: *Science*, v. 246, p. 103–107.
- Robinson, P.T., Walker, G.W., and McKee, E.H., 1990, Eocene (?), Oligocene, and lower Miocene rocks of the Blue Mountains region: *Geology of the Blue Mountains region of Oregon, Idaho, and Washington*: U.S. Geological Survey Professional Paper 1437, p. 29–62.
- Robyn, T.L., 1979, Miocene volcanism in eastern Oregon: An example of calc-alkaline volcanism unrelated to subduction: *Journal of Volcanology and Geothermal Research*, v. 5, p. 149–161.
- Rytuba, J.J., and McKee, E.H., 1984, Peralkaline ash-flow tuffs and calderas of the McDermitt volcanic field, southeast Oregon and north central Nevada: *Journal of Geophysical Research*, v. 89, p. 8616–8628.
- Rytuba, J.J., and Vander Meulen, D.B., 1991, Hot-spring precious metal system in the Lake Owyhee volcanic field, Oregon-Idaho, in Raines, G., Lisle, R.E., Schaffer, R.W., and Wilkinson, W.H., eds., *Geology and ore deposits of the Great Basin*: Geological Society of Nevada Symposium Proceedings, v. 2, p. 1085–1096.
- Shotwell, J.A., 1963, The Juntura Basin—Studies in Earth history and paleoecology: *American Philosophical Transactions*, v. 53, part 1, 77 p.
- Sisson, T.W., and Grove, T.L., 1993, Experimental investigations of the role of H<sub>2</sub>O in calc-alkaline differentiation and subduction zone magmatism: *Contributions to Mineralogy and Petrology*, v. 113, p. 143–166.
- Sleep, N.H., 1997, Lateral flow and ponding of starting plume material: *Journal of Geophysical Research*, v. 102, p. 10,001–10,012.
- Streck, M.J., Johnson, J.A., and Grunder, A.L., 1999, Field guide to the Rattlesnake tuff and High Lava Plains near Burns, Oregon: *Oregon Geology*, v. 61, no. 3, p. 64–76.
- Swanson, D.A., Wright, T.L., Hooper, P.R., and Bentley, R.D., 1979, Revisions in stratigraphic nomenclature of the Columbia River Basalt Group: *U.S. Geological Survey Bulletin* 1457-G, 59 p.
- Swanson, D.A., Anderson, J.L., Camp, V.E., Hooper, P.R., Taubeneck, W.H., and Wright, T.L., 1980, Reconnaissance geologic map of the Columbia River Basalt Group, northern Oregon and western Idaho: U.S. Geological Survey Open-File Report 81–797, scale 1:250,000.
- Swanson, D.A., Wright, T.L., Camp, V.E., Gardner, J.N., Helz, R.T., Price, S.M., Reidel, S.P., and Ross, M.E., 1981, Reconnaissance geological map of the Columbia River Basalt Group, Pullman and Walla Walla quadrangles, southeast Washington and adjacent Idaho: U.S. Geological Survey Miscellaneous Investigations Series Map I-1139, scale 1:250,000.
- Swisher, C.C., Ach, J.A., and Hart, W.K., 1990, Laser fusion <sup>40</sup>Ar/<sup>39</sup>Ar dating of the type Steens Mountain Basalt, southeastern Oregon and the age of the Steens geomagnetic polarity transition: *Eos (Transactions, American Geophysical Union)*, v. 71, p. 1296.
- Takahashi, E., Nakajima, K., and Wright, T.L., 1998, Origin of the Columbia River basalts: Melting model of a heterogeneous mantle plume head: *Earth and Planetary Science Letters*, v. 162, p. 63–80.
- Thompson, R.N., and Gibson, S.A., 1991, Subcontinental mantle plumes, hotspots, and preexisting thinspots: *Geological Society [London] Journal*, v. 148, p. 973–977.
- Tolan, T.L., Reidel, S.P., Beeson, M.H., Anderston, J.L., Fecht, K.R., and Swanson, D.A., 1989, Revisions and estimates of the areal extent and volume of the Columbia River Basalt Group, in Reidel, S.P., and Hooper, P.R., eds., *Volcanism and tectonism in the Columbia River flood basalt province*: Geological Society of America Special Paper 239, p. 1–20.
- Tuttle, O.F., and Bowen, N.L., 1958, Origin of granite in the light of experimental studies in the system NaAlSi<sub>3</sub>O<sub>8</sub>-KAlSi<sub>3</sub>O<sub>8</sub>-SiO<sub>2</sub>: *Geological Society of America Memoir* 75, 153 p.
- Vallier, T.L., 1995, Petrology of pre-Tertiary igneous rocks in the Blue Mountains region of Oregon, Idaho, and Washington: Implications for the geologic evolution of a complex island arc, in Vallier, T.L., and Brooks, H.C., eds., *Geology of the Blue Mountains region of Oregon, Idaho, and Washington*: Petrology and tectonic evolution of pre-Tertiary rocks of the Blue Mountains region: U.S. Geological Survey Professional Paper P-1438, p. 125–209.
- Walker, G.W., 1977, Geologic map of Oregon east of the 121st meridian: U.S. Geological Survey Miscellaneous Investigations Map I-902, 1:500,000 scale.
- Walker, G.W., 1979, Revisions to the Cenozoic stratigraphy of Harney Basin, southeastern Oregon: *U.S. Geological Survey Bulletin* 1475, 35 p.
- Walker, G.W., and MacLeod, N.S., 1991, Geologic map of Oregon: U.S. Geological Survey special map, scale 1:500,000.
- Walker, G.W., and Swanson, D.A., 1968, Summary report on the geology and mineral resources of the Harney Lake and Malheur Lake areas of the Malheur National Wildlife Refuge, north-central Harney County, Oregon: U.S. Geological Survey Bulletin 1260-L, 17 p.
- Weinberg, R.F., 1997, Rise of starting plumes through mantle of temperature-, pressure-, and stress-dependent viscosity: *Journal of Geophysical Research*, v. 102, p. 7613–7623.

MANUSCRIPT RECEIVED BY THE SOCIETY 6 AUGUST 2001  
 REVISED MANUSCRIPT RECEIVED 25 FEBRUARY 2002  
 MANUSCRIPT ACCEPTED 1 JULY 2002

Printed in the USA